Autonomous Sensor Insertion and Exchange for Cornstalk Monitoring Robot

Janice Seungyeon Lee

CMU-RI-TR-24-73

December 1, 2024

The Robotics Institute
School of Computer Science
Carnegie Mellon University
Pittsburgh, PA

Thesis Committee:
Professor Oliver Kroemer
Professor George Kantor
Dr. Abhisesh Silwal
Moonyoung Lee

Submitted in partial fulfillment of the requirements for the degree of Master of Science in Robotics.

Abstract

Interactive sensors are an important component of robotic systems but often require manual replacement due to wear and tear. Automating this process can enhance system autonomy and facilitate long-term deployment. We developed an autonomous sensor exchange and maintenance system for an agriculture crop monitoring robot that inserts a nitrate sensor into cornstalks. A novel gripper and replacement mechanism, featuring a reliable funneling design, were developed to enable efficient and reliable sensor exchanges. To maintain consistent nitrate sensor measurement, an on-board sensor maintenance station was integrated to provide in-field sensor cleaning and calibration. While enabling the sensor exchange capabilities of this corn monitoring robot, the autonomous insertion capabilities was enhanced through two-finger gripper design and compliant soft-pads in the gripper finger tips along with position-based visual servoing implementation. The system was deployed at the Ames Curtis Farm in June 2024, where it successfully inserted nitrate sensors with high accuracy into 30 cornstalks with a 77% success rate.

Acknowledgments

I would like to express my deepest gratitude to those who have supported me throughout this journey.

First and foremost, I extend my heartfelt thanks to my advisors, Prof. Oliver Kroemer and Prof. George Kantor, whose guidance, encouragement, and expertise have been invaluable. Their mentorship has been pivotal in shaping my academic growth and research.

I am also deeply grateful to the members of the IAM Lab for their camaraderie, insightful discussions, and unwavering support. Their feedback and collaboration have been a constant source of inspiration. A special thanks to Moonyoung Lee for the mentorship and support throughout the project.

To the Kantor Lab members, thank you for your knowledge-sharing, collaborative spirit, and the many ways you have contributed to my development as a researcher. I am especially grateful to Francisco Yandun, Srini Vijayarangan, Ruiji Liu, and Chuck Whittaker for their assistance during field tests and throughout the development process.

I would like to express my sincere appreciation to the NIMO team—Thomas Detlefsen, Shara Lawande, Saudamini Ghatge, Shrudhi Ramesh Shanthi, and Sruthi Mukkamala—for their dedicated contributions to this project. I also wish to extend my thanks to our collaborators at Iowa State University whose expertise and partnership have greatly enriched this work. The success of this project is a testament to the combined efforts, shared knowledge, and unwavering commitment of everyone involved.

Finally, I owe the deepest thanks to my family. Their unconditional love, patience, and support have been my foundation, motivating me to persevere and complete this work.

Funding

This work was supported in part by NSF Robust Intelligence 1956163 and NSF/USDA-NIFA AIIRA AI Research Institute 2021-67021-35329.

Contents

When this dissertation is viewed as a PDF, the page header is a link to this Table of Contents.

List of Figures

List of Tables

Chapter 1

Introduction

1.1 Motivation

In recent years, the agricultural industry has witnessed a significant transformation with the integration of advanced sensing technology and robotics. This shift towards precision agriculture aims to optimize the use of resources, improve crop yields, and enhance profitability, addressing the growing global demand for food and shortage of labor [3, 34]. Autonomous robotic systems equipped with advanced sensors can perform a wide range of tasks, from planting and harvesting to irrigation and pest control, increasing productivity and reducing labor costs. Additionally, real-time data collection through sensors can provide farmers with detailed insights into the needs of their crops, allowing them to make informed decisions regarding irrigation, fertilization, and pest management.

In this thesis, a robotic system was developed to automate the labor-intensive and repetitive task of monitoring nitrate levels in cornstalks, a key indicator of crop health and the fertilizer use. By inserting contact-based sensors into the plants, the system provides real-time data on nitrate level, which indicates the amount of fertilizer absorbed by the cornstalk. This automation enhances efficiency, allows more frequent monitoring, and helps farmers make timely decisions on fertilizer use, promoting sustainable farming and optimizing crop yields.

The robotic system operates by inserting contact-based sensors directly into the cornstalks. Interactive sensors, such as tactile sensors and physical probes, are an

Figure 1.1: Crop Monitoring: (a) Manual monitoring (b) Autonomous robot system monitoring

important component for robots collecting data from their environment. The ability to acquire data during interactions allows a robot to observe information about objects that it would not be able to detect using only passive sensor observations. However, interactive sensors often experience extensive wear and tear that requires them to be replaced on a regular basis. This exchanging of sensors is often performed manually by a human operator, which limits the overall autonomy of the robot system and its ability to be deployed for extended periods of time. Therefore, developing an autonomous solution for sensor replacement is crucial to enhancing the longevity and autonomy of robotic systems in agricultural environments.

The main task of this robotic system is inserting the sensor into multiple cornstalks to collect nitrate levels across different stalks in the field and exchanging the sensor. To achieve this goal efficiently and accurately, the system must be able to handle the complexities of real-world environments. Field conditions, such as plant variability, wind, and uneven terrain, make it difficult for pre-programmed robotic motions to achieve accurate sensor placement. Visual servoing uses real-time visual feedback to dynamically adjust the robot's movements, ensuring precise sensor insertion without damaging the plants. This approach enhances the robot's ability to operate autonomously in unpredictable conditions, improving sensor placement accuracy and overall system reliability.

1.2 Objective

This research explores the challenges of improving the sensor insertion reliability, creating an autonomous sensor exchange and enhancing the adaptability to the dynamic field environment for an agriculture robot monitoring cornstalks. The robot is tasked with forcefully pushing a sensor into cornstalks in the field to measure their nitrate readings for informed fertilizer usage. Sensor technology developed by Ali et al [12] is used for the system. This sensor has two electrodes printed on a PCB with electrochemical layers applied on top that converts nitrate concentration to voltage (see [12] for details). The focus of this research is in creating the infrastructure needed to repeatedly deploy multiple of such sensors reliably in the field without additional human intervention.

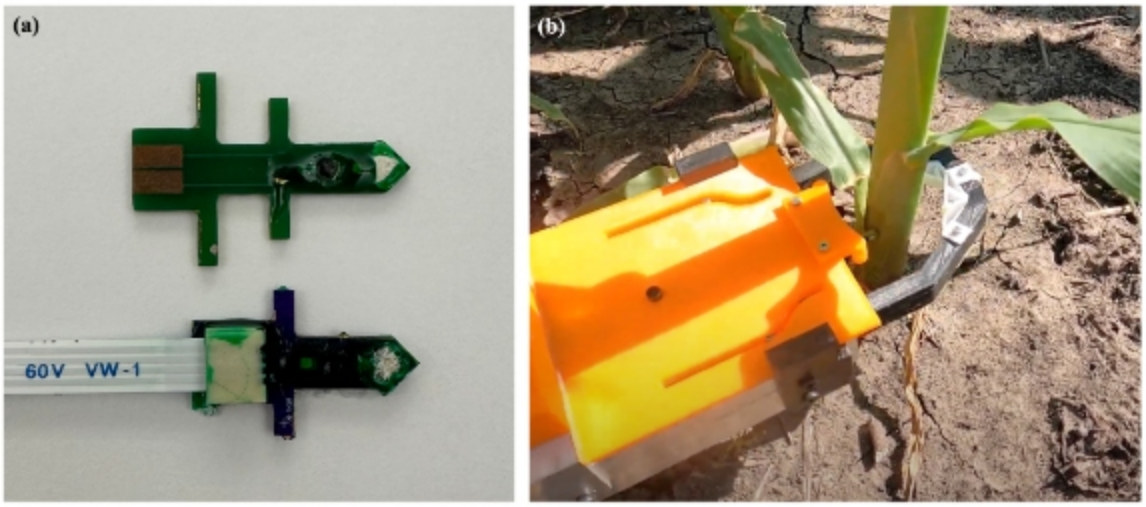

Figure 1.2: Sensor Insertion: (a) Nitrate Sensor (b) Gripper inserting sensor

This research's approach includes three core components. First, a gripper was designed to insert the contact-base sensor into cornstalks and to engage and disengage with the sensor both mechanically and electronically. Secondly, a station was developed for removing expired sensors and housing replacement sensors in a precise and accessible manner using a physical funneling approach. Lastly, a visual servoing controller was implemented for the robotic manipulator to align the gripper to the center of the stalk to improve sensor insertion success. Although the focus is on the nitrate sensor, many of the underlying principles of our system can also be adopted

for other physical sensors that requires autonomous exchange and is tasked with precise insertion.

The three components are described in Sections 4, 5, and 6 respectively, following overviews of the related work (Section 2) and the system requirements (Section 3). For each component we provide design details and insights needed to have the sensor insertion and exchanges occurring reliably. The robotic system is evaluated both in the lab and in the field, with results elaborated in Section 7.

Chapter 2

Related Work

2.1 Sensors and Robots in Agriculture

Precision agriculture has recently been using advancement of sensing technology and robotics to optimize resources and improve yields and profits [3, 34]. A variety of sensing technologies are employed in agricultural applications, including vision-based sensing [9] for applications such as structural characterization [18, 26] and plant detection [17, 22], as well as interactive sensors for soil [1, 13] and crop monitoring [12]. These sensors are integrated with robotic systems to improve autonomy for labor-intensive and repetitive agricultural tasks such as monitoring [36], harvesting [7] and management [37]. In this research, a robotic system was developed to insert contact-based sensor for cornstalk monitoring and to autonomously replace, clean and calibrate the sensors in the field for long-term deployment.

2.1.1 Nitrogen Sensing

Nitrogen is a critical nutrient for plant growth and a key indicator of soil fertility and crop health. While fertilizers provide essential nutrients for plant growth, using too much fertilizers can harm not only the plants, but also the soil and the surrounding ecosystem, resulting in problems such as fertilizer burn, soil acidification and nutrient pollution. Therefore, accurate, rapid, and cost-effective nitrogen sensing is essential for optimizing fertilizer use, understanding nitrogen loss patterns, and advancing

precision agriculture while protecting the environment [32].

Traditional methods, such as soil sampling and destructive plant analysis, are labor-intensive and lack real-time data capabilities. Soil sampling offers a snapshot of soil nitrogen content but lacks real-time monitoring capabilities [23], while destructive plant analysis, such as extractions of dried plant materials, disrupts the field and is unsuitable for ongoing assessments [25]. In contrast, in-stalk nitrogen sensing offers a non-destructive and continuous alternative for monitoring nitrogen levels directly within plants [12]. This approach can provide real-time feedback on plant health and nutrient uptake, enabling more precise interventions such as targeted fertilizer applications. By integrating in-stalk nitrogen sensing with autonomous robotic systems, it becomes possible to gather high-resolution data across large fields efficiently, improving both the sustainability and profitability of agricultural practices.

2.2 Gripper Design

Grippers are crucial end-of-arm tools for robotic manipulation, facilitating interaction with environments and objects [38]. Specially for grasping objects, two-finger designs are often used for their simplicity [5, 24]. The two-finger design can be actuated for inserting task utilizing a linear actuator and sliding tracks to enable both insert and grasp motion [28]. Gripper are often customized for tool-switching function, involving mechanical [2] and electrical engagement [31]. This research presents a novel gripper capable of reliable autonomous sensor exchange while maintaining effective grasping and insertion capabilities.

2.3 Precise Alignment

Sensor exchange necessitates precise alignment and insertion, particularly for small-sized sensors. Guo et al. developed an intelligent robotic hand equipped with multiple small sensors for tolerant electronic connector mating [6]. Gregorio et al. used computer vision and tactile sensor for wire terminal insertion [8]. Morgan et al. introduced combined vision-based object tracking, compliant manipulation, and learned hand models to accomplish tight-tolerance peg-in-hole insertions [27]. For a

mechanical solution, Nie et al. proposed a gripper design with an L-shaped finger that acts as a guide for aligning [29]. This research explores a novel mechanical solution using a simple and cost-effective funneling mechanism that only involves minimal changes to the gripper design.

2.4 Visual Servoing

Visual servoing is a control strategy that uses feedback from visual information to guide robotic motions [11]. In precise insertion tasks, it plays a critical role in ensuring precise alignment and insertion by dynamically adjusting the robot's movements in response to visual input [33]. There are two primary types of visual servoing: image-based (IBVS) and position-based (PBVS) [35]. IBVS directly uses image features, such as key points or edges, to compute control actions, and PBVS relies on estimating the full 3D position of the object relative to the robot using the camera data [15]. In agricultural robotics, visual servoing has been applied to tasks such as fruit picking [4] and harvesting [30]. However, its application in autonomous sensor insertion for agricultural applications remains limited. This research leverages position-based visual servoing for real-time guidance of the robotic manipulator during stalk grasp and sensor insertion to ensure accurate placement and adjust to the dynamic field conditions.

2.5 Prior Lab Work

This research builds upon a succession of prior work in the lab focused on grippers and robotic systems for agricultural applications. Jenkins developed a gripper used for grasping sorghum stalks, similarly for contact-base sensing (Fig. 2.1(a)) [16]. Notably, this gripper has two-finger design and uses sliding mechanism both to manipulate the fingers and to insert sensor. Lee et al. developed the previous gripper design for the cornstalk monitoring robot, which used a stereo camera for stalk detection [21] (Fig. 2.1(b)).

Prior work also has been done in developing the robotic system for cornstalk nitrate monitoring [10, 21] (Fig. 2.1 (c)). In this previous iteration, the robot inserts a sensor

into a stalk, and the sensor is deployed with a data logger unit for long term data collection of 30 days (Fig. 2.1 (d)). This approach has two limitations. First, the data is collected after 30 days, which is not fully leveraging the advantage of the sensor's real-time data collection capabilities. Secondly, the sensor deployment requires a human operator to reload a new sensor and data logger unit for every insertion, which significantly reduces autonomy and scalability. Through these limitations, this narrows the research problem to:

1. Could the robotic system insert the sensor into multiple cornstalks to enable real-time data collection?
2. Is it possible to enable autonomous sensor exchange to enhance autonomy for long-term field deployment?

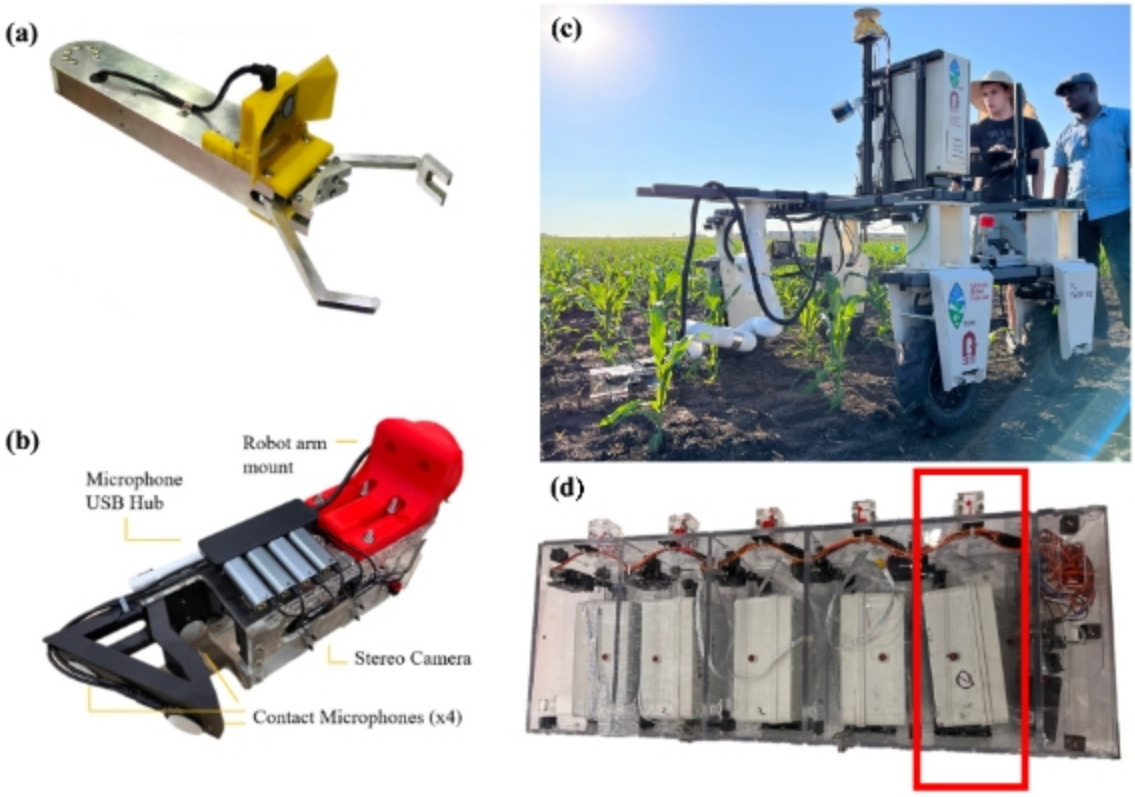

Figure 2.1: Prior Work: (a) Two-finger gripper (b) Previous gripper design (c) Previous iteration of cornstalk monitoring robot (d) Sensor data logging unit

Building upon prior work, the research problems were addressed by developing a robotic system capable of precise, autonomous sensor insertion and exchange. The main contributions of this thesis are:

- Development of a custom gripper using a single-actuator coupled sliding mechanism for stalk grasping, sensor inserting, and sensor exchanging
- Reliable high-precision sensor replacement for low-precision robot manipulator using cost-effective funneling mechanism
- Development of visual servoing controller for precise sensor insertion into cornstalks
- Evaluation of the robot system on real-world cornstalks with multiple sensors in field condition.

Chapter 3

Problem Statement

3.1 Robotic System Overview

The primary application goal of this research is the development of a robotic system that inserts a nitrate sensor into multiple cornstalks and is capable of replacing and maintaining the sensors between insertions, for autonomous crop monitoring. The robotic system consists of five subsystems: (i) a mobile base for navigating in the field, (ii) a robotic arm for manipulating the gripper to target cornstalks or to sensor calibration and replacement mechanisms, (iii) a gripper for inserting sensors into cornstalks, (iv) a replacement mechanism for exchanging sensors, and (v) a sensor calibration mechanism for calibrating and cleaning the sensors (Fig. 3.1). The robot operates with an Intel i9-processor with RTX4070 GPU and utilizes ROS framework.

3.2 Sensor Insertion

To ensure accurate sensor readings during sensor insertion, the sensor must be inserted at least 8.5mm into the cornstalk's pith region. The nitrate sensor consists of a flat spike that is 5mm wide, 12mm long, and 1.6mm thick. Two electrodes are located on one side of the spike along the central axis, 3mm from the tip and 5.5mm apart [12]. The sensor needs to be inserted fully covering both of the electric nodes, which corresponds to an insertion depth of 8.5mm, as shown in Fig. 3.2 (a). Also, the

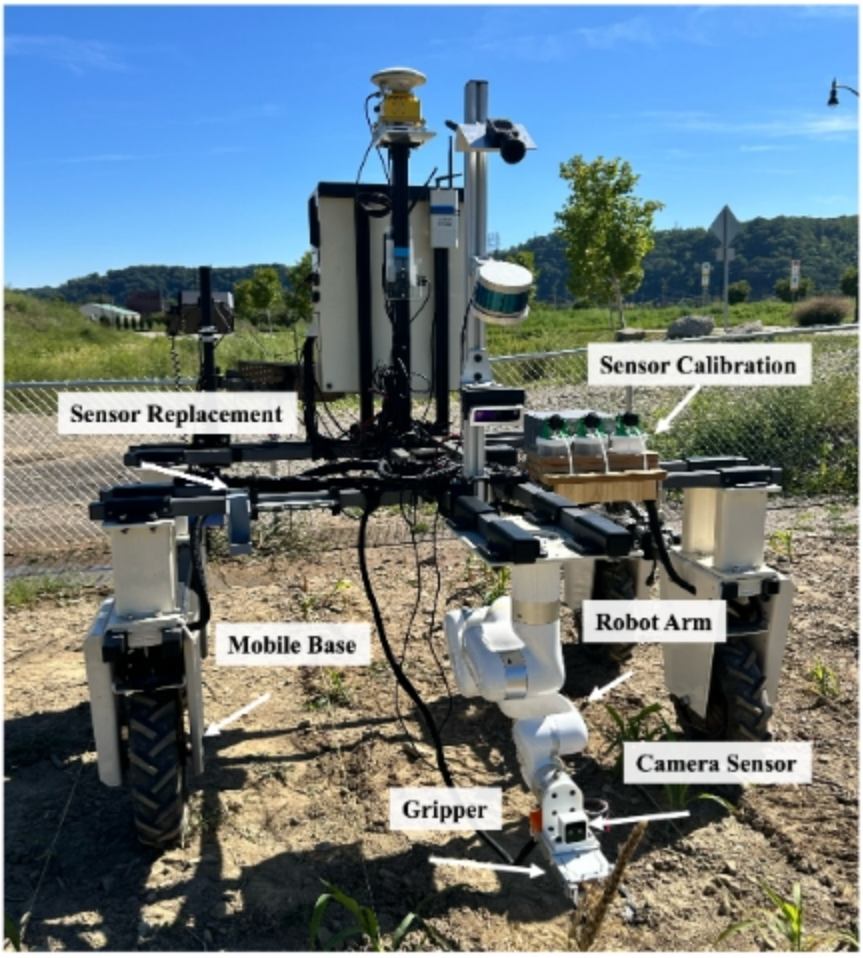

Figure 3.1: Robotic System Overview

sensor must be inserted within the pith region of the cornstalk, which can be achieved by inserting the sensor 1.3 cm to 2.5 cm above the ground. The nitrate concentrate decreases by 4% for every centimeter deviation above the ground [14] (Fig. 3.2 (c)). These depth and height requirements needs to be satisfied for the robot to get accurate and consistent sensor measurements.

3.3 Sensor Replacement and Maintenance

A single sensor is used for multiple insertions to collect readings across various cornstalks in a field. However, the nitrate sensor has chemical layers on top of the

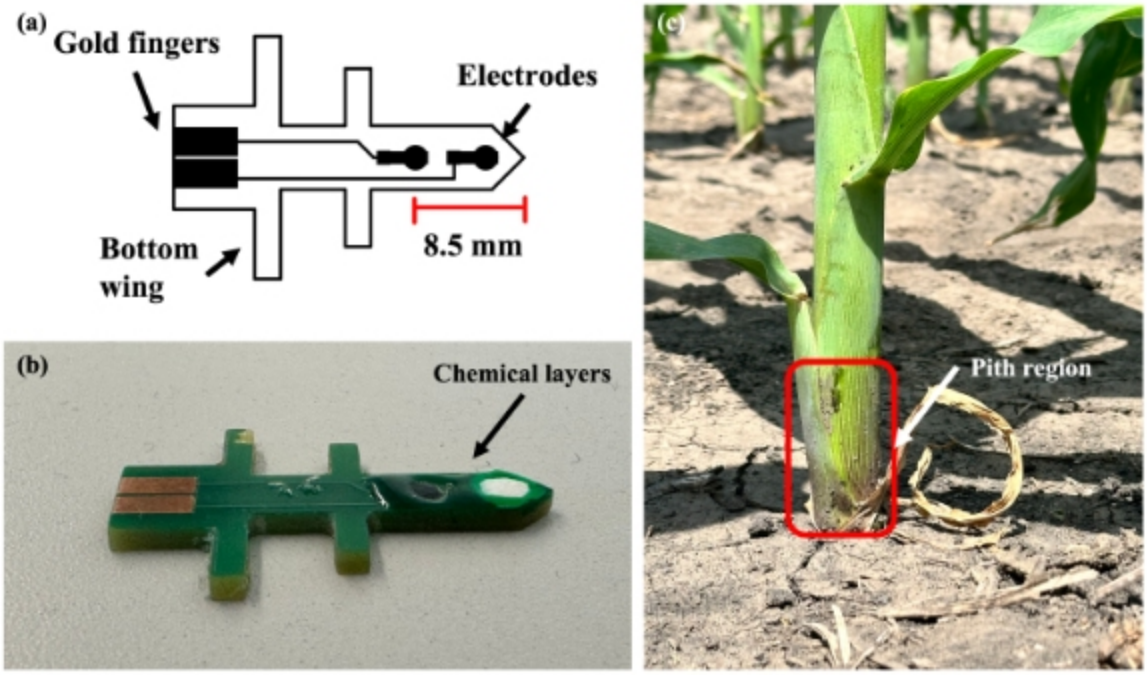

Figure 3.2: Sensor Requirements: (a) Sensor diagram (b) Chemical layers of the sensor (c) Pith region of the cornstalk

electrodes which utilizes a unique photosensitive epoxy bioresin [12], and these layers are prone to defects after repeated penetrations (Fig. 3.2 (b)). As a result, the sensor must be replaced periodically—typically after every five to ten plant insertions—to ensure reliable readings. Exchanging sensors does not only involve replacing the sensor itself, but each sensor must also be calibrated and cleaned in the field for consistent measurements and extended use. The electromechanical properties of the sensor system [12] can vary with each insertion, necessitating calibration and cleaning before every use. Cleaning is particularly important to avoid contamination of the calibration solutions with dirt or cross-mixing, as this could compromise data integrity.

3.4 Field Conditions

The variability of cornstalks in field environments presents specific requirements for the robotic system and its gripper, which must adapt to diverse shapes and diameters

ranging from 15 mm to 35 mm [19]. Field conditions, such as plant variability, wind, and uneven terrain, make it difficult for pre-programmed robotic motions to achieve accurate sensor placement. However, for a reliable sensor insertion, it is crucial for the sensor to be align to the vertical center of the corn prior to insertion. To achieve efficient and accurate sensor placements in the face of challenges such as plant variability and the unpredictability of field conditions, the system must be equipped with gripper design to accommodate the variation in stalk diameter and advanced control strategies capable of navigating these complexities in real-time.

Figure 3.3: Cornstalks in the field

Chapter 4

Gripper Design

4.1 Design Motivation

A gripper was developed to achieve sensor insertion into cornstalks of various size and shape using a two-finger design with soft pads. This gripper is also capable of autonomously exchanging the sensors utilizing a coupled sliding mechanism.

The gripper was custom designed to satisfy the requirements stated in Section 3. The gripper needs to accommodate a wide range of cornstalk diameter and be able to align the stalk to the center. In addition, the gripper needs to be compact in size to grasp stalks in cluttered environment and is required to exchange sensors. To address these requirements, the gripper uses two-finger design to grasp on to cornstalk with various size and shape, and the soft pads on the finger tips assist with aligning to the center. The coupled sliding mechanism uses pin slots to convert linear actuator movement to rotational motion for the fingers and the sensor lever to enable sensor insertion and replacement while remaining compact in size. These gripper mechanisms and design choices are explained more in detail in the following section.

4.2 Gripper Mechanisms

The gripper has an overall dimension of 9cm x 10cm x 28cm (HxWxD). As shown in Fig. 4.1, the gripper has a two-finger design [28] for grasping, and each of the finger

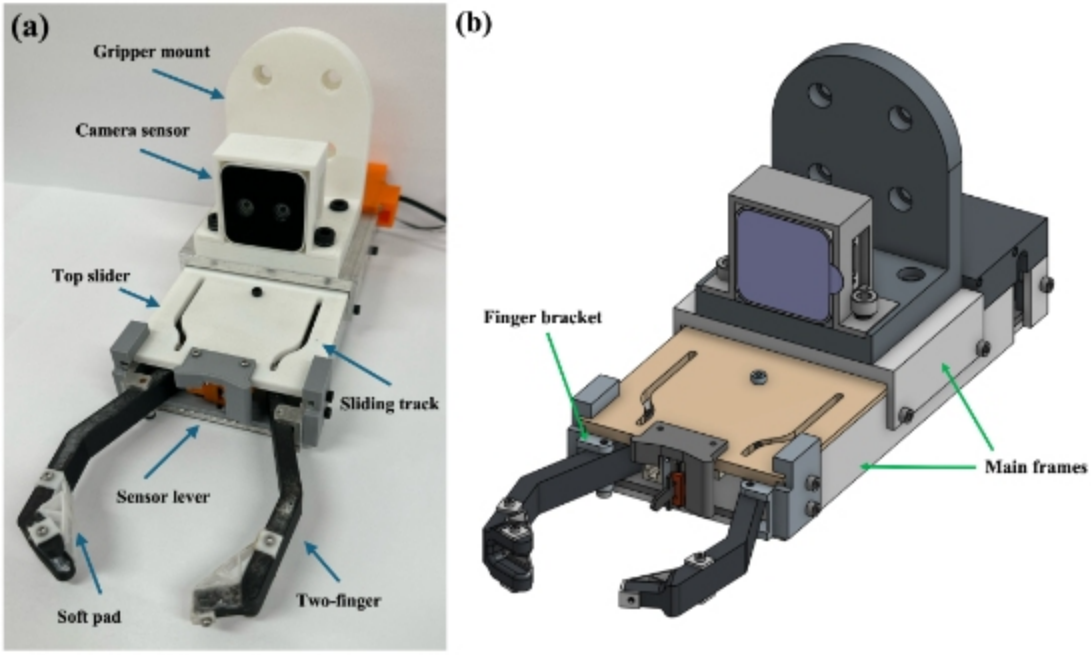

Figure 4.1: Gripper Design: (a) Hardware (b) CAD design

tips has a custom soft pad to help align the stalk to the center of the gripper. The camera is placed on top of the gripper facing forward for detecting cornstalks. The gripper uses a 50 mm stroke linear actuator from Actuonix to grasp stalks, and insert and exchange sensors. The main frames and the finger brackets that have large forces applied were fabricated using aluminum. Other parts, such as the fingers, lever and slider, that require specific customized features were 3D printed using PLA filament.

4.2.1 Two-finger Design

The two-finger gripper is designed to efficiently navigate to the target stalk in a straight line with the camera sensor facing the same direction. This approach reduces positional errors resulting from changing orientation or direction and the risk of colliding with adjacent stalks. On each of the finger-tips, a custom soft pad was attached to form a v-shape when grasping, which assists in aligning the stalk while being capable of grasping a wide range of stalk diameters. The soft pads is able to grasp relatively thick stalks since it is deformable, and for the thin stalks, the pads push the stalk towards the center during the grasping process. These soft pads were

3D printed using TPU filament.

4.2.2 Coupled Sliding Mechanism

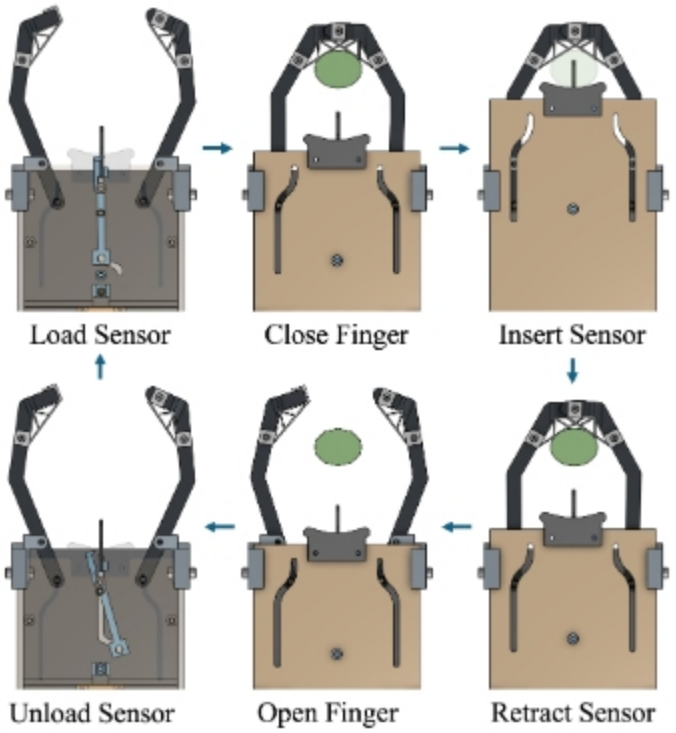

Figure 4.2: Coupled Sliding Mechanism

The gripper is actuated with one linear actuator that utilizes a coupled sliding mechanism. This mechanism enables three motions: (i) opening and closing the fingers for grasping stalks, (ii) inserting the sensor into the grasped stalk, and (iii) loading and unloading the sensor (see Fig. 4.2). The finger and sensor lever motions are based on the extended length of the linear actuator.

As shown in Fig. 4.4, there are two different sliding tracks where one on the bottom plate is for the sensor lever and the one on the top slider is for the finger movement. While the bottom plate remains stationary attached to the main frame, the top slider is connected to the linear actuator and slides forward. The finger pins attached to the inner end of the fingers slides through the finger tracks leading to the finger grasping and sensor insertion motions, as shown in Fig. 4.3. For the sensor

Figure 4.3: Gripper motion for grasping the stalk and inserting sensor.

lever motion, the pin at the end of the sensor lever moves along the lever pin track located on the bottom plate. As the lever pivots when the slider is moving forward, it hooks the sensor in the sensor slot located in the front of the top slider and unloads the sensor when the linear actuator retracts fully (see Fig. 4.2). In Fig. 4.4, each proportion of the slide tracks for the sensor lever pin and the finger pins corresponds to 1) moving the sensor lever 2) opening and closing finger 3) inserting and retracting the sensor.

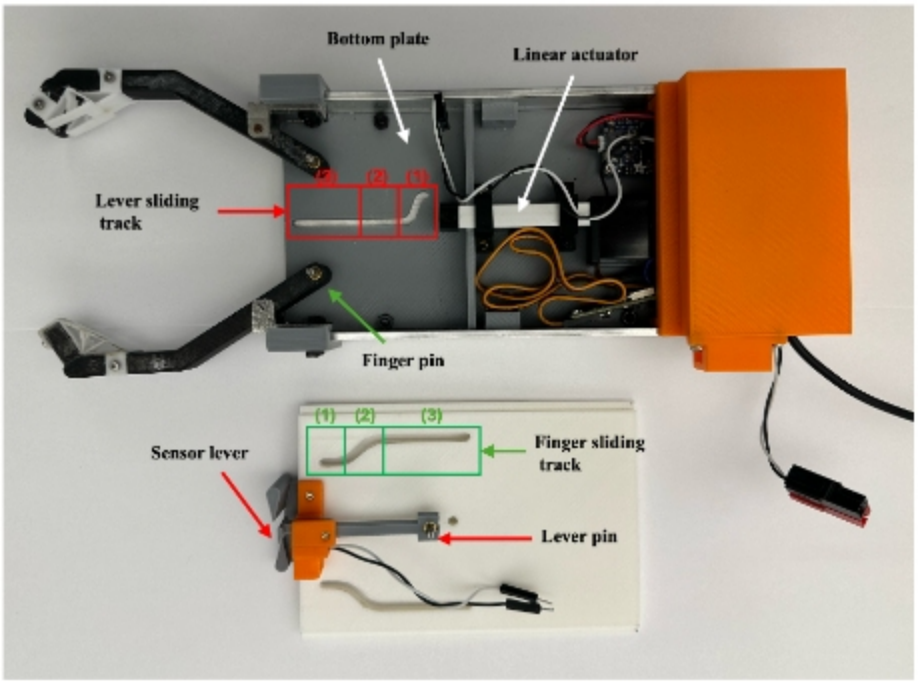

Figure 4.4: Coupled Sliding Mechanism Hardware

4.3 Fabrication

The gripper's fabrication prioritized durability and functionality, particularly for components subjected to high stress. The main frame and the brackets responsible for holding the two fingers were milled from aluminum to ensure strength and rigidity, as the gripper interacts with cornstalks and encounters obstacles like the ground. Initially, 3D printing was used for rapid prototyping to allow for multiple fast design iterations and to test various parameters, such as finger shape and length, track length distribution and sensor size. This iterative design process was essential due to the nature of this inner-connective gripper design. But, during the insertion tests in the lab and field, the printed parts were not strong enough to withstand the applied forces, which can be up to 30N. This part failures, as shown in Fig. 4.5(a), prompted the switch to metal fabrication for the key components that needed to withstand the large force but did not require custom shapes and size. The metal-fabricated parts include the main frames and finger bracket (see Fig. 4.1, 4.5).

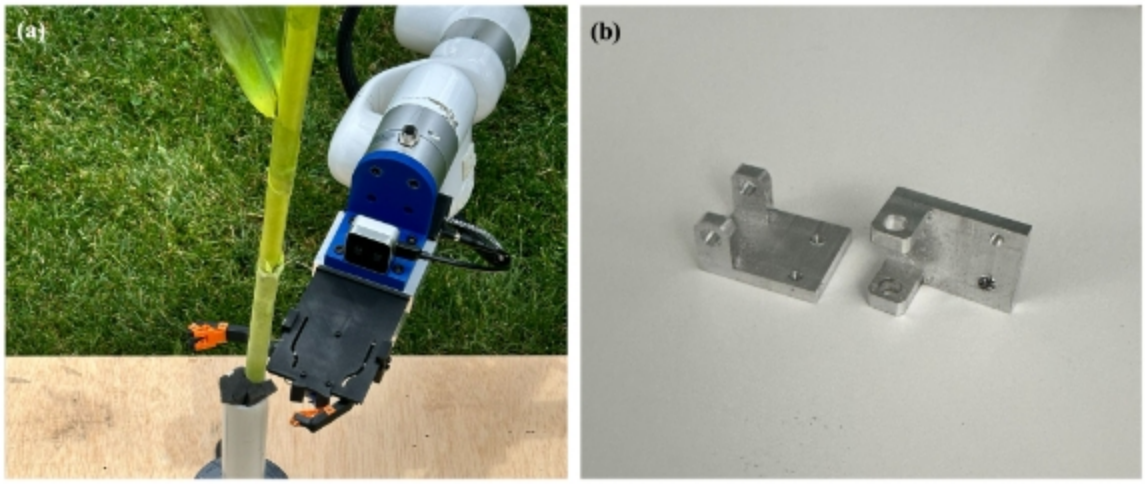

Figure 4.5: Gripper Fabrication: (a) Gripper finger bracket failing during testing (b) Metal fabricated finger bracket

Other parts, which required customized shapes and specific functionalities, were 3D-printed. The top slider, featuring the finger sliding track, and the bottom plate, which housed the lever sliding track and electronic components (linear actuator, Adafruit Feather 32u4, nitrate sensor ADC, Adafruit PowerBoost, and Adalogger

FeatherWing), were designed for precise integration (See Fig. 4.6). The fingers, gripper mount, and electronics cover were also 3D-printed to match these specifications. Smaller parts, like the sensor holder and lever, required tight tolerances and were similarly 3D-printed. The soft pads at the fingertips, inspired by tire designs, were 3D-printed using TPU filament for flexibility and deformation.

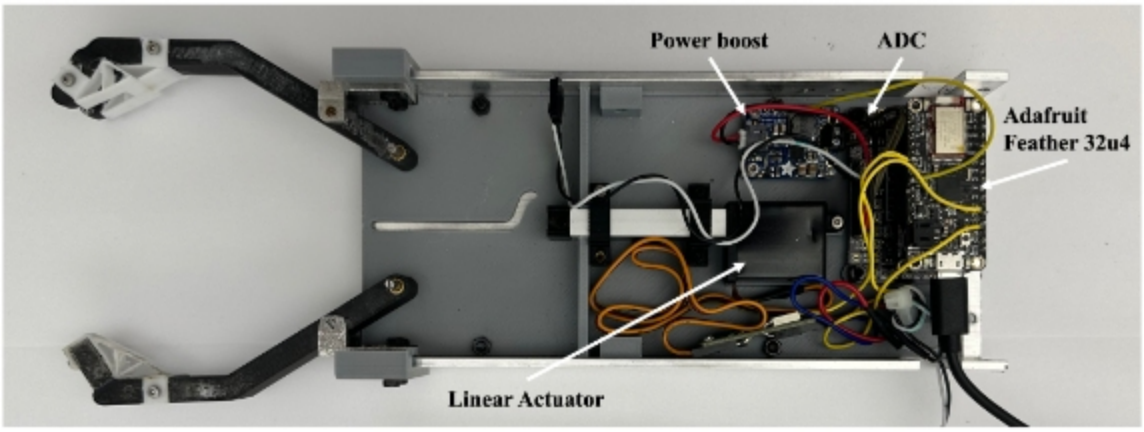

Figure 4.6: Gripper Electronics

Assembly involved using heated threads for 3D-printed parts and metal threads with screws for stronger, stable connections, ensuring a balance between rapid prototyping and structural integrity.

4.4 Broader Application

The coupled sliding mechanism can be adapted to actuate other grippers, particularly those designed for tasks involving contact-based sensing. Below are instructional guidelines for implementing the coupled sliding mechanism:

1. **Define Problem Requirements and Constraints.**

   Begin by identifying the specific requirements and constraints for the application. For instance, in this study, the gripper required a force of $F_{\text{insert}} = 30\,\text{N}$ for insertion, with the cornstalk diameters ranging from $d_{\min} = 15\,\text{mm} = 0.59\,\text{in}$ to $d_{\max} = 35\,\text{mm} = 1.4\,\text{in}$. Additionally, the gripper design needed to maintain a compact form factor.

2. **Select an Appropriate Linear Actuator.**

   Choose a linear actuator based on the defined requirements. For the compact gripper in this study, the actuator needed to deliver at least 30 N of force with a stroke length exceeding 35 mm to accommodate sensor insertion. Note, $d_{\max} = 35mm$ is the length required for the sensor insertion. For applications requiring finger opening and sensor hooking, a stroke length between $1.5\,d_{\max}$ and $2\,d_{\max}$ is recommended.

   For this gripper, the Actuonix P8-P Micro Linear Actuator (50mm, 165:1, 12V) was selected. If higher force is required and compactness is less critical, a ball screw actuator could be a viable alternative.

3. **Design Finger Geometry.**

   Design the gripper fingers by considering the distance between them (gripper width), the size and shape of the target object, and the actuator's stroke length. The finger geometry should securely grasp the object and meet the functional requirements of the task. The fingers must open wider than $d_{\max}$ and provide sufficient clearance to securely hold the object after closing, leaving adequate space for sensor insertion (Fig. 4.7). Specifically, when the fingers are closed and the object is grasped, there must be at least d_{insert} remaining to allow for sensor insertion.

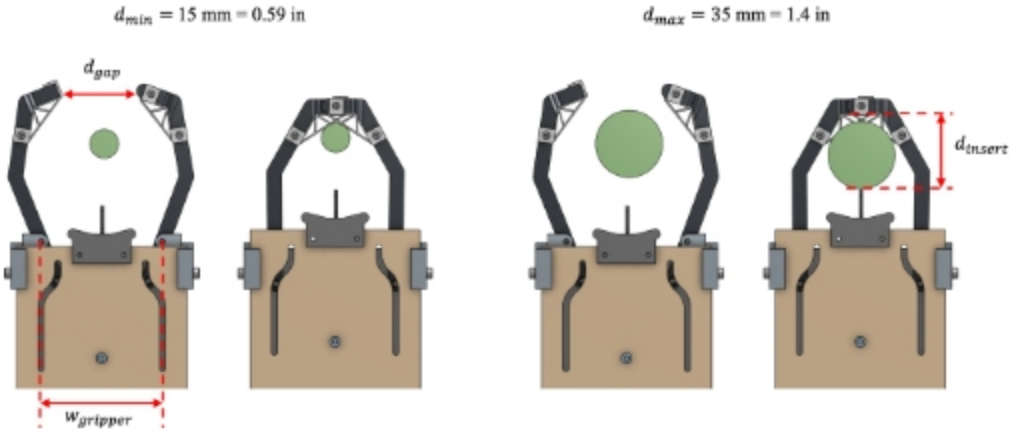

Figure 4.7: Gripper Finger Design Parameters

For this gripper, the design parameters are as follows:

(1) $d_{\text{open}} = 1.78\,\text{in}$, which exceeds $d_{\max}$, providing sufficient space to accommodate large cornstalks during the grasping motion, given the gripper width constraint of $w_{\text{gripper}} = 2.49\,\text{in}$.

(2) The insertion clearance is set to $d_{\text{insert}} = 1.55\,\text{in}$, ensuring adequate space for insertion while accommodating large cornstalk diameters.

Figure 4.8(a) illustrates the detailed finger design and key parameters. The finger geometry can be simplified into two key length parameters relative to the pivot: l_{finger} (finger length) and l_{pivot} (pivot arm length). When the finger rotates (blue path) around its pivot, it forms a triangular relationship as shown in Fig. 4.8(c). This relationship can be expressed as:

$$\frac{d_{\max}}{2} + tol_{\text{clearnace}} : l_{\text{finger}} = x_{\text{track}} : l_{\text{pivot}}$$

where x_{track} is the horizontal length of the finger track described in the next step. Here, $\frac{d_{\max}}{2} + tol_{\text{clearnace}}$ and l_{finger} are fixed values, while l_{pivot} and x_{track} can be adjusted while maintaining the defined ratio.

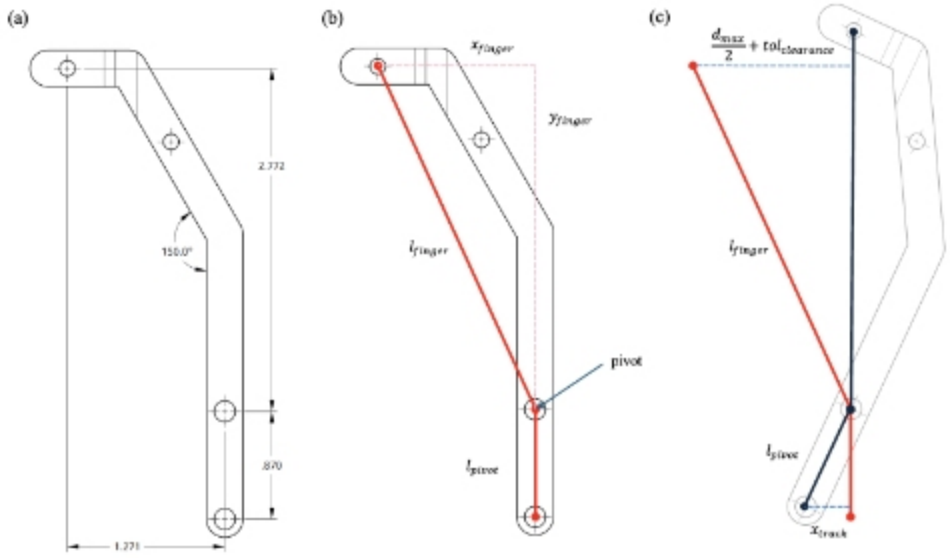

Figure 4.8: Gripper Finger Design Diagram

4. **Design Finger Track.**

   With the finger geometry established, the finger track on the top slider needs to be designed (see Fig. 4.9). The track incorporates three distinct movement regions:

   - d_{hook}: The length allocated for hooking and unhooking the sensor.
   - d_{open}: The length used for opening and closing the fingers.
   - d_{insert}: The length dedicated to inserting the sensor.

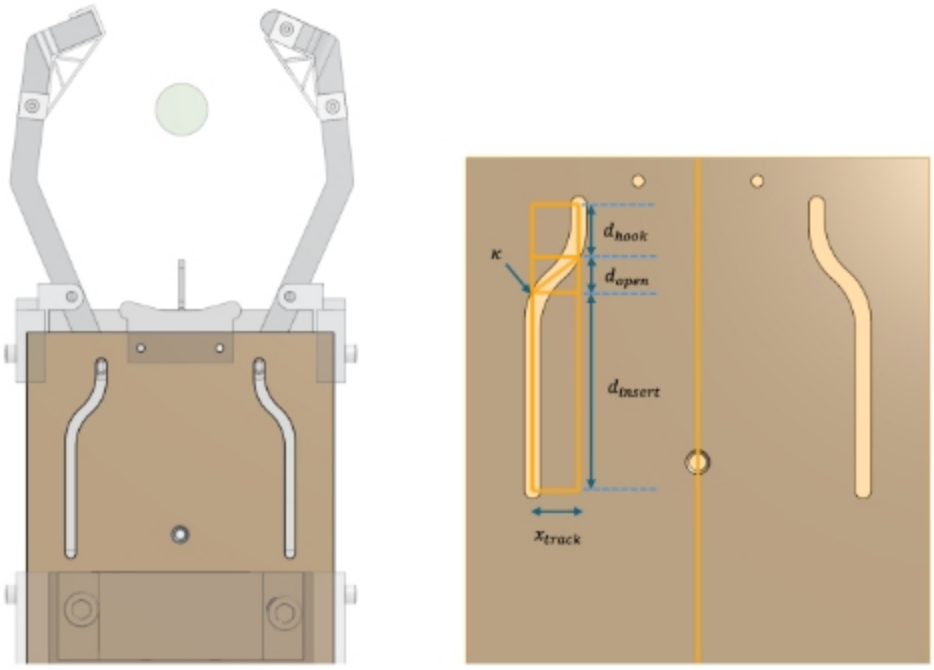

Figure 4.9: Finger Track Design Parameters

The total slider length is constrained by the stroke length of the linear actuator, with d_{insert} determined by the $d_{\max}$ requirement. The values of d_{hook} and d_{open} must be adjusted within the available length (stroke length $- d_{\text{insert}}$).

It is critical to balance these parameters, especially d_{open}. Excessive d_{open} reduces the length available for sensor hooking, potentially impeding this motion. Also, insufficient d_{open} may cause the pin slot of the finger to jam in the sliding track due to an overly steep slope.

The angular displacement of the finger motion is governed by x_{track} (as shown

in Fig. 4.8(c)), and d_{open} should be tuned to ensure the pin moves smoothly through the track. Factors affecting pin motion include pin material, slider material, friction, and the linear actuator's power.

Additionally, κ defines the curvature of the slope in the d_{open} region of the track. Proper selection of κ is essential to achieving smooth and consistent finger motion.

5. **Iterative Parameter Adjustment.**

   The following parameters are refined through iterative design to optimize performance: l_{pivot}, x_{track}, d_{open}, d_{hook}, and κ.

Chapter 5

Funneling Mechanism for High-precision Alignment

5.1 Autonomous Sensor Exchange

One sensor is used for multiple insertions to collect readings across multiple cornstalks within a field. However, after multiple forceful penetrations into stalks, the chemical layers on top of the sensor is subject to potential damage. To address this issue, the sensor needs to be replaced with a new sensor periodically. We replace the sensor after every 5 plant insertions.

To enable autonomous exchange of the sensor, first the sensor needed to be modified. The sensor originally had a ribbon cable connection, but these type of wire connections are tricky for replacement. Therefore, the sensor was modified to have gold finger enabling contact-based electric connection. From the gripper side, the gripper's design also had to take into consideration the sensor replacement. The gripper needed to be able to engage with the sensor electronically and mechanically. To connect electronically, the gripper uses a small-scale battery connector for the contact-based connection. For the mechanical engagement, the gripper utilizes a lever mechanism that grips on the sensor securely for the forceful insertion into the cornstalks and also pushes out the sensor for replacement process. Through the hardware customization of the sensor and the gripper, the gripper is capable

of holding on to the new sensor and exerting the old sensor for autonomous sensor replacement.

With the sensor and gripper modified and designed to engage electrically and mechanically, another important aspect of the sensor exchange is precise alignment. When a new sensor needs to be loaded, the sensor has to be placed precisely in the tight sensor slot (Fig. 5.2) located in the gripper. This requires the gripper to precisely align itself to the sensor, which is very challenging using low-precision gripper and manipulator. This challenge was addressed using the funneling mechanism. Developing the funneling mechanism along with the sensor modification and the sensor lever enable reliable autonomous sensor exchange.

5.2 Sensor Modification

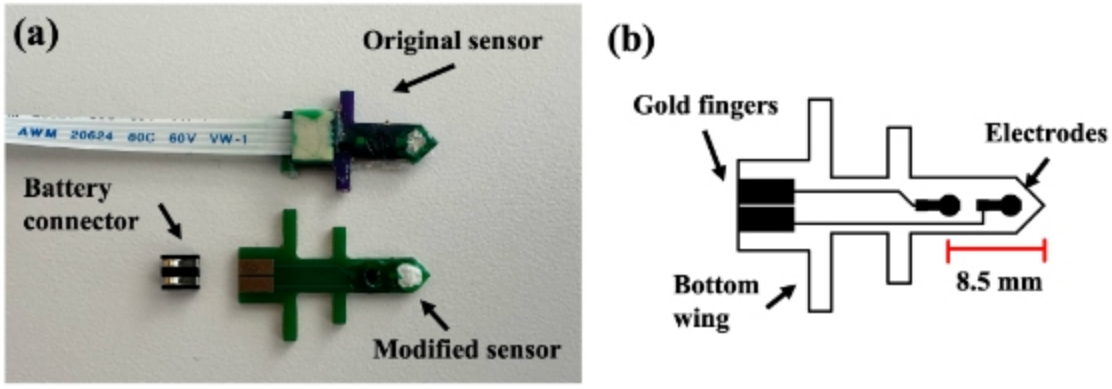

Figure 5.1: Modified Sensor: (a) Modified sensor compared with original sensor (b) Electrical diagram of the sensor

To elaborate on the sensor modification, the sensor was modified to have contact-based electrical connections and an additional wing shape to allow it to be mechanically hooked and secured. The original nitrate sensor utilized a ribbon cable for electrical connection. However, to allow reliable loading and unloading by the gripper, the sensor was modified to incorporate a contact-based electrical interface using gold finger connections, as shown in Fig. 5.1(b). As the sensor is inserted in the sensor slot of the gripper, it makes contact-based connection with the battery connector, which interfaces with the on-board electronics for reading the sensor. Our modified

sensor also has two wings, and the additional wing is used for the sensor lever to hook on to for a strong mechanical engagement when retracting the sensor from the sensor holder and the stalk.

5.3 Lever Mechanism for Loading Sensor

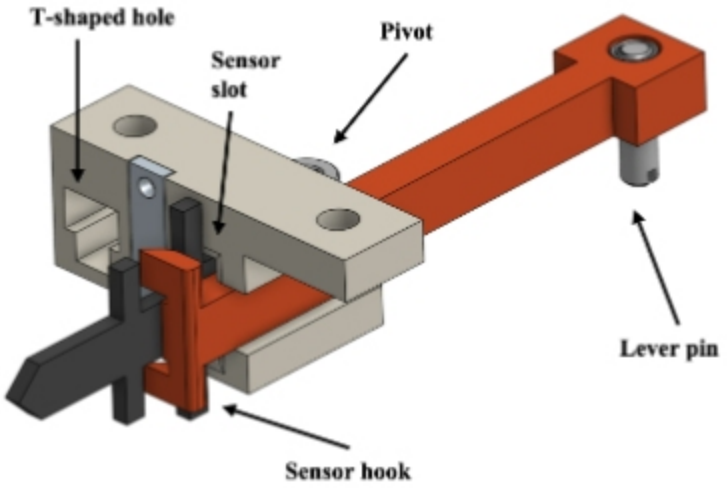

Figure 5.2: Sensor Lever

As shown in Fig. 5.2, the gripper employs a lever mechanism to securely engage with the sensor, ensuring robust mechanical locking. Inserting and retracting the sensor in corn are force-intensive tasks, requiring up to 30N of force. Therefore, it is crucial that the sensor remains firmly secured when loaded. The sensor slot, mounted at the front end of the top slider, moves linearly along with the linear actuator. The lever pivots as the lever pin advances along the sensor lever sliding track located in the bottom plate of the gripper (Fig. 4.4), effectively locking the sensor in place during high-force operations.

When the linear actuator fully retracts, the lever disengages, allowing the sensor slot to move inward toward the gripper's main frame. At this point, the bottom wing of the sensor contacts the metal frame, forcing the sensor out of the slot. This lever mechanism not only ensures secure engagement during sensor insertion but also facilitates sensor ejection upon retraction.

5.4 Funnel Mechanism for Aligning Sensor

When loading a new sensor, the sensor needs to be aligned accurately to the sensor slot on the gripper due to a submillimeter tolerance. The sensor slots have tight fit for the sensor because it establishes contact-based electrical connection and the lever mechanical engagement. The surface area of the electrical contacts on the sensor is 2.2mm x 5mm (WxH) which necessitates submillimeter precision for alignment. However, the sensor slot on the gripper is located on the top slider (Fig 4.1) along with the sensor lever. The top slider slides along the top of the gripper frame to hook sensor lever to load a new sensor (refer to 4.2.2), and to reduce friction resistance the motion has low precision. To address the low-precision, a funneling mechanism was implemented for aligning the sensor closely to the sensor slot.

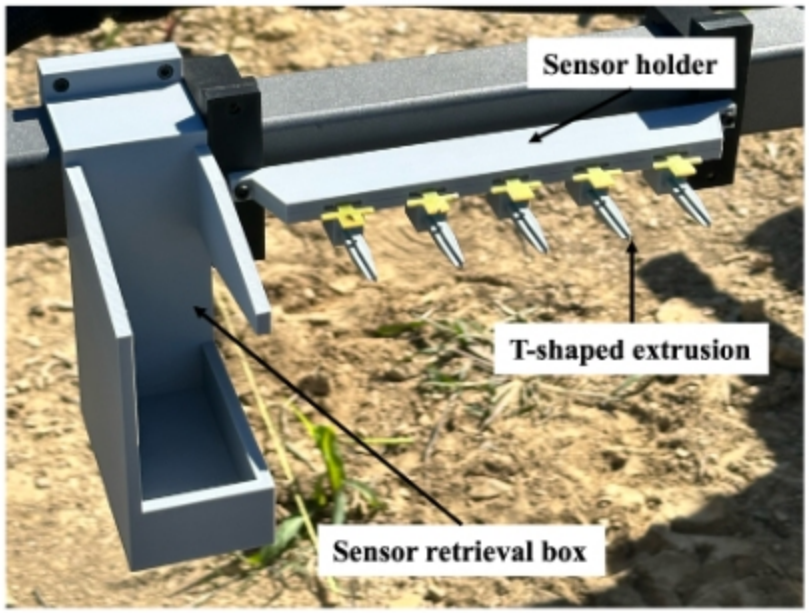

Figure 5.3: Sensor Replacement Mechanism

The sensor replacement mechanism, placed on the right front bar of the AMIGA base (Fig. 5.3), consists of a sensor holder that holds 5 five sensor in a known location and a sensor retrieval box. The sensor holder has sensors placed in each individual slot with a tapered T-shaped extrusion below it. This T-shaped extrusion is used to align the sensor slot prior to loading the sensor by funneling it into the T-shaped hole on the gripper adjacent to the sensor slot (Fig. 5.4. The end of the T-shape

extrusion starts with 18 % of the original surface area and expands. This allows the sensor holder and the gripper to engage with higher tolerance, and as the surface area expends, it aligns the sensor slot perfectly prior to loading the sensor. Without the funneling, the gripper is not capable of the submillimeter precision alignment, often resulting in collision and gripper damage. This funneling approach can be expanded to other application that requires high-precision alignment of the gripper or manipulator for various sensor or tool switching purposes.

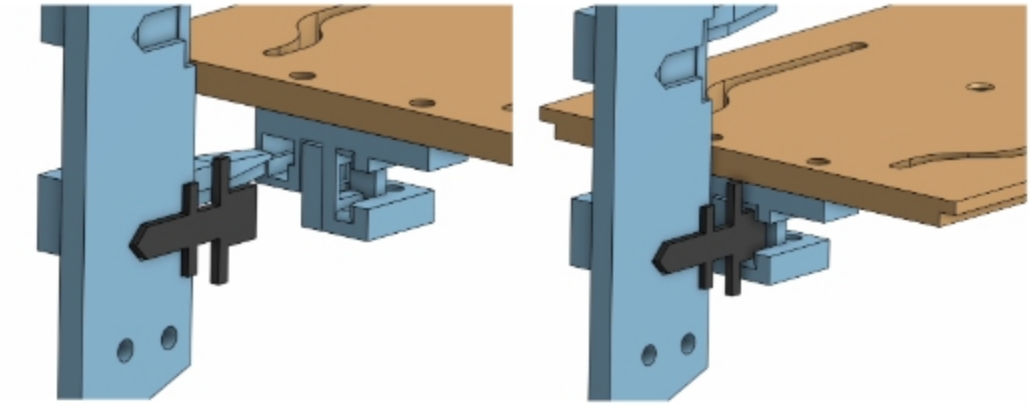

Figure 5.4: Sensor Exchange Funneling

5.5 Replacement Motion Sequence

Figure 5.5: Replacement Motion Sequence

For the sensor replacement, the arm initially moves toward the sensor replacement mechanism. The gripper facing sideways moves toward the sensor retrieval box, and the linear actuator is retracted fully to open up the sensor lever. As the sensor slot in the gripper is retracted the sensor wing hits the main metal frame, forcing the sensor out of the slot. The unloaded sensor drops into the box below for retrieval.

The gripper moves sideways to intentionally hit the flat surface plate located between the box and the sensor holder to ensure that the sensor is removed from the gripper for the edge cases where the sensor is stuck. Due to the forceful sensor insertions into cornstalks, the sensor often becomes stuck in the sensor slot. Once the slot is emptied out, the gripper reaches to the sensor holder for a new sensor. The sensor is aligned by funneling the T-shaped extrusion. Once the sensor is aligned into the sensor slot, the sensor lever hooks on to the sensor and the arm moves outward to retract the sensor from the sensor holder. The sensor holder contains 5 sensors and therefore can do 5 replacements, but can be easily extended to hold more sensors.

5.6 Sensor Calibration

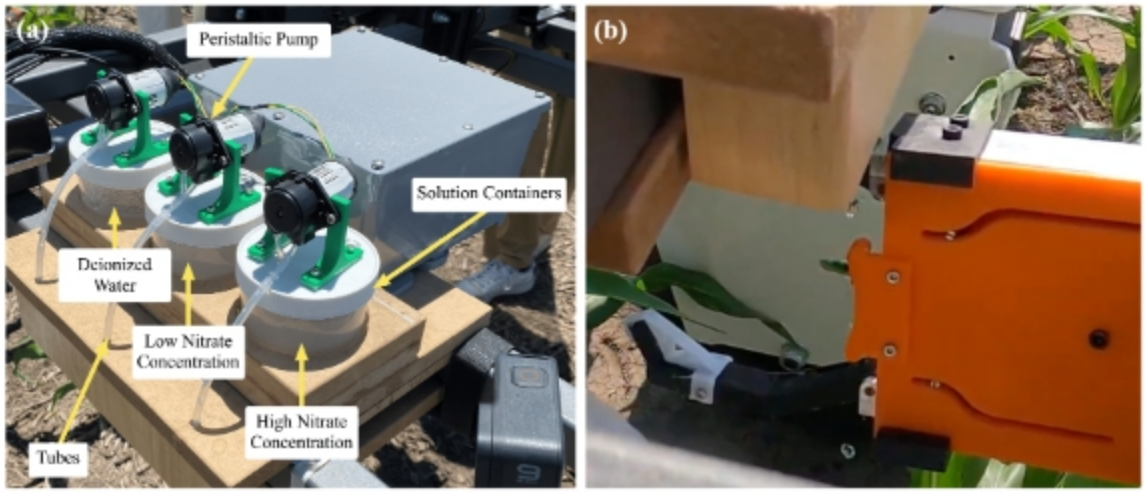

Figure 5.6: Sensor Calibration Mechanism: (a) Unit mounted on the base (b) Solution dripping onto the sensor

To enable autonomous sensor exchange, an on-board autonomous sensor calibration system is required to ensure accurate sensor reading for every sensor insertion. Prior to each insertion, the nitrate sensor undergoes a cleaning and calibration process. The nitrate sensor uses an epoxy bioresin that varies in response from sensor to sensor and thus requires calibration before use [12]. The sensor calibration mechanism, shown in Fig. 5.6 (a), consists of three containers holding solutions with different concentrations of nitrate solution: deionized water (0 ppm), 200 ppm and 2000 ppm.

Each container has a 5V DC peristaltic pump connected with a tube that provides a dripping flow of solution. For the calibration process, the robotic arm positions the gripper such that the sensor is placed under the extended tubes to ensure the flow of solution directly onto the sensor electrodes (see Fig 5.6 (b)).

Nitrate sensor calibration is conducted using two-point calibration given the two solutions of known concentration. The sensor is exposed to the low and high concentration nitrate solutions, and the corresponding voltage readings are recorded. From this calibration, interpolation can be created based on the linear relationship of the nitrate concentration and voltage for this nitrate sensor [12]. The sensor is cleansed with deionized water before and after calibration to remove any contaminants.

5.7 Significance of the Replacement Mechanism

The funneling-based sensor replacement mechanism ensures reliable, high-precision alignment during sensor exchanges, compensating for minor gripper misalignments and preventing collisions. By allowing submillimeter alignment without the need for extremely high-precision gripper movements, this mechanism ensures reliable and repeatable sensor exchanges in field operation. The simple but effective combination of a tapered extrusion and a matching-shaped hole in the gripper allows the system to compensate for the misalignments, preventing collisions that could damage the gripper or the sensor.

This funneling approach is not only robust in field conditions but also highly adaptable. It could be expanded for various use cases beyond agricultural sensing. For example, in industrial automation, similar mechanisms could be employed to facilitate the automatic switching of tools or sensors, ensuring precision without the need for highly sophisticated, expensive gripper technologies. In medical robotics, such a mechanism could aid in the autonomous replacement of surgical instruments, improving efficiency and safety in operating rooms. Additionally, in household robotics, this mechanism support tasks such as inserting keys and charging cables by ensuring precise alignment and reliable insertion.

Another key advantage of this system is that it requires minimal modifications. A small tapered hole on the gripper and a corresponding extrusion on the tool or sensor holder are sufficient to enable precise alignment. This makes the funneling

mechanism a cost-effective solution that can be widely applied to various robotic manipulation tasks where tool or sensor switching is necessary.

In summary, the sensor replacement mechanism not only enhances the functionality of the cornstalk monitoring robot by ensuring the durability and precision of sensor exchange but also serves as a versatile tool-switching method that could be adapted to a wide range of industries requiring similar high-precision manipulation.

Chapter 6

Visual Servoing for Stalk Alignment

The visual servoing approach was implemented to achieve precise alignment between the gripper and the cornstalk's vertical center, enabling accurate sensor insertion in unstructured, variable field environments. Previous open-loop control methods used a single, initial stalk position for insertion; however, in dynamic settings, external factors—such as mobile base shifts and occlusions from plant leaves—often resulted in misalignment with the stalk. To address these challenges, a closed-loop visual feedback control system was introduced, allowing the gripper to iteratively adjust its position based on real-time perception updates. This adaptive approach enhances the robot's ability to consistently align with the stalk's centerline, proving essential for reliable and autonomous manipulation in precision agriculture.

The visual detection system extends the prior work by Lee et. al [21] through incorporating stalk width estimation to optimize the insertion angle and implementing visual servoing control strategy for maximizing sensor insertion success.

6.1 Visual Detection and Initial Positioning

The visual detection system aims to accurately identify the optimal 3D location for sensor insertion on the cornstalk. To achieve this, Intel RealSense D405, an RGB-D camera sensor, captures the stalks, which are then detected in the image using a

segmentation model. A 3D line is fitted to the resulting mask, and any invalid stalks are filtered out to refine detection accuracy.

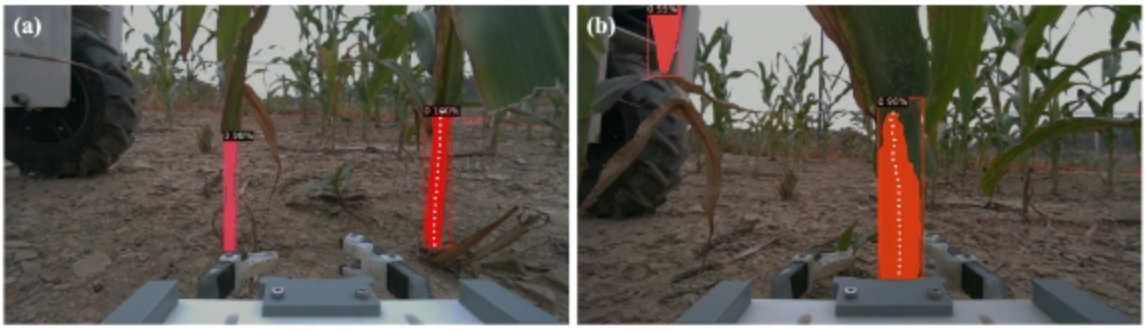

Figure 6.1: Visual Detection: (a) Initial Stalk Detection (b) Stalk Position Update

For segmentation, this system utilizes the Mask-R-CNN architecture, trained on a custom dataset of 2,667 RGB images captured approximately 15 cm above the ground. These images were labeled with Meta's Segment Anything model [20], generating segmentation masks from which feature points were extracted. The feature points are centered horizontally along each stalk and spaced equidistantly based on a tunable hyperparameter. Using RANSAC, a line is then fitted to these 3D points. The designated grasp point is positioned a fixed distance, controlled by a hyperparameter, from the stalk base. This grasp point is either accepted or rejected depending on its location, the segmentation model's confidence, and the measured width of the stalk.

Stalk width detection is achieved by fitting a 2D line to the feature points on the RGB image. Rows of pixels perpendicular to this line are analyzed using the depth mask to confirm they belong to the stalk, after which the pixel widths are calculated. The median width value is converted into a real-world measurement using the stalk's median depth and the camera's intrinsic parameters.

The visual servoing phase begins by calculating the cornstalk's current position based on detected points along its length, averaging these points to ensure accurate alignment. This averaging helps mitigate any discrepancies caused by environmental conditions or the inherent structural variability of plant stalks.

6.2 Closed-Loop Visual Servoing with Adaptive Displacement Control

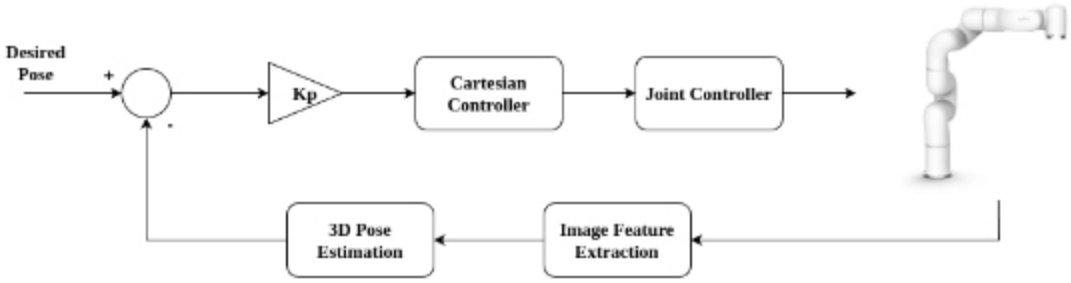

Figure 6.2: Position-based Visual Servoing Controller

Once the stalk's initial position is established, the gripper's coordinates are determined relative to the manipulator base, serving as a reference for the alignment adjustments. The gripper then iteratively aligns to the stalk center using updated stalk location detected to gradually minimizes the distance between the gripper and stalk. This process ensures that the system maintains precise alignment despite environmental dynamics.

The visual servoing loop continues until the gripper's distance to the cornstalk center falls within a set tolerance, which was 5 mm. During each iteration, the algorithm determines the required adjustments along the x- and y-axes by calculating the positional discrepancy between the detected stalk and gripper position. This positional error is scaled by a proportional gain factor, set as $k_p = 0.25$, producing incremental displacements that direct the gripper closer to the stalk's vertical axis.

1. **Stalk Center Calculation:** The coordinates of the stalk center are computed as the average of detected grasp points:

$$x_{\text{stalk}} = \frac{1}{n}\sum_{i=1}^{n} x_i, \quad y_{\text{stalk}} = \frac{1}{n}\sum_{i=1}^{n} y_i \tag{6.1}$$

   where n is the number of grasp points detected.

2. **Displacement Vector:** The displacement vector between the gripper and

stalk center is:

$$\Delta x = x_{\text{stalk}} - x_{\text{gripper}}, \quad \Delta y = y_{\text{stalk}} - y_{\text{gripper}} \tag{6.2}$$

3. **Distance:** The Euclidean distance to the target is:

$$d = \sqrt{\Delta x^2 + \Delta y^2} \tag{6.3}$$

4. **Proportional Gain:** The proportional gain is applied to avoid overshoot of the robot:

$$\Delta x_{\text{incre}} = k_p \cdot \Delta x, \quad \Delta y_{\text{incre}} = k_p \cdot \Delta y \tag{6.4}$$

5. **Convergence Condition:** The servoing loop terminates when the distance is below the target tolerance:

$$|d| < d_{\text{tolerance}} \tag{6.5}$$

6. **Stalk Switch Condition:** If the detected distance exceeds the maximum limit, the loop terminates to avoid aligning with the wrong stalk:

$$|d| > d_{\text{max}} \tag{6.6}$$

7. **Position adjustment:** The calculated Δx_{incre} and Δy_{incre} is applied to the robot manipulator for positional adjustment. The gripper's position is updated after each motion command using the robot information from the manipulator.

These calculated displacements are then applied to adjust the gripper's position accordingly. After each adjustment, the gripper's updated coordinates are retrieved, becoming the reference for the next iteration. This incremental correction mechanism enables the system to handle minor disturbances, ensuring a smooth and stable alignment process that maintains accuracy without abrupt changes that could compromise the system's control. This approach, which iteratively refines the gripper's positioning relative to the stalk, is well-suited for dynamic field conditions, allowing the robotic system to achieve reliable alignment in unstructured agricultural environments.

6.3 Robustness and Error Mitigation

The implementation integrates comprehensive error-handling protocols to ensure reliability during visual servoing, especially in dynamic and uncertain field environments. If the perception module is unable to consistently detect the cornstalk, an error is logged, and the process halts to prevent unintended operations or alignment errors. To mitigate potential issues related to misidentifying the target stalk, the algorithm checks that the distance to the stalk center remains within a defined threshold, which was set as 25 cm. Should this distance exceed the threshold, the system interprets it as a shift to a different stalk, safely stopping the alignment procedure to maintain accuracy.

6.4 Adapting PBVS for Other Applications

The PBVS framework can be generalized for other robotic applications requiring visual servoing, such as pick-and-place operations, object tracking, or assembly tasks. By adapting the control parameters, sensor inputs, and target criteria, the same principles can guide a manipulator to align with or interact with a desired object in dynamic environments.

This pseudocode outlines the general procedure for implementing PBVS in different applications. The specific functions for detecting the target, acquiring sensor input, and commanding manipulator movement will depend on the hardware and software stack used in the system. The iterative approach ensures the manipulator adjusts incrementally, maintaining precision and robustness across a wide range of tasks.

Algorithm 1 PBVS Implementation

procedure PBVS CONTROLLER($camera feed, k_p, d_{\text{tolerance}}, d_{\max}$)
    Initialize gripper position: $gripper_x$, $gripper_y$
    while True **do**
        Detect target position:
            $target_x, target_y \leftarrow$ COMPUTE TARGET COORDINATES(camera feed)
        Calculate positional error:
            $error_x \leftarrow target_x - gripper_x$
            $error_y \leftarrow target_y - gripper_y$
        Compute Euclidean distance:
            $d \leftarrow \sqrt{error_x^2 + error_y^2}$
        if $d < d_{\text{tolerance}}$ **then**
            return "Alignment Successful"
        else if $d > d_{\max}$ **then**
            return "Target Not in Valid Range"
        end if
        Calculate incremental movements:
            $delta_x \leftarrow k_p \cdot error_x$
            $delta_y \leftarrow k_p \cdot error_y$
        Apply movement command:
            $gripper_x \leftarrow gripper_x + delta_x$
            $gripper_y \leftarrow gripper_y + delta_y$
        Update target detection and repeat.
    end while
end procedure

Chapter 7

System Evaluation

7.1 Robotic System

This chapter presents the evaluation of the robotic system's performance in autonomously inserting sensors into cornstalks across multiple waypoints. The system includes the mobile robot platform (AMIGA), the manipulator arm (xARM), and custom-built components for sensor insertion, cleaning, calibration, and replacement. This chapter provides a detailed discussion of the AMIGA mobile base and the xARM robotic manipulator, highlighting their roles and integration within the robotic system.

7.1.1 Robot Platform AMIGA

The AMIGA, a commercially available all-electronic micro-tractor, was customized and used as the mobile base of the system. The base was adapted to fit the dimensions of the cornfield [10]. At the testing site, the cornstalks were planted in rows with row spacing of 75 cm and were at the growth stage between V6 - V7 which has the average height of 60 cm. Thus, the dimension of the AMIGA base was set to be 150 cm x 86 cm (W x H) to provide clearance.

To drive to the field and to cornstalks at different waypoints autonomously, a navigation system was developed to enable barn-to-field and in-row navigation. The barn-to-field navigation drives the AMIGA platform from an in-door barn to the

testing site. This barn-to-field navigation works not only from the barn but when it is initiated at an arbitrary location along the path. The in-row navigation drives the AMIGA within the rows to preselected waypoints for sensor insertion. In the case where there are no cornstalks available or reachable in the waypoint, the navigation moves forward for known distance, which was 10m, to search for other available cornstalks. Once the insertion process is complete, the navigation system moves to the next waypoint. This navigation system enabled the robotic system to drive autonomously to the field testing site and in between the waypoints during testing.

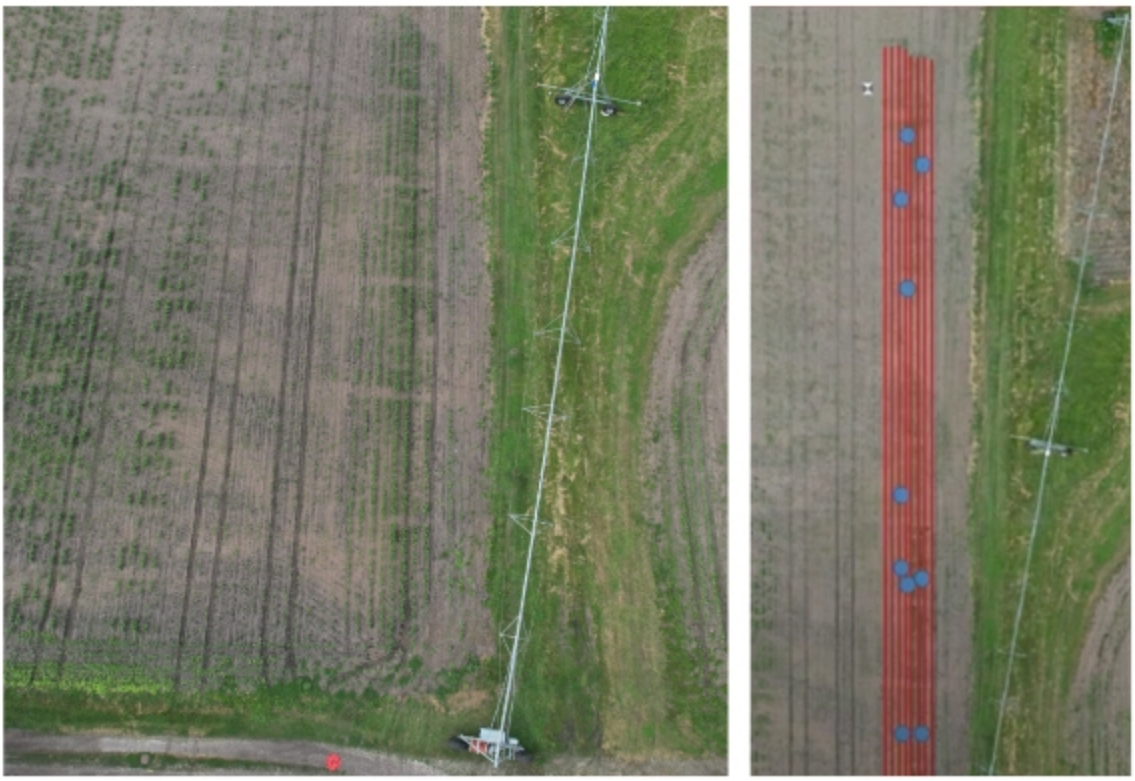

Figure 7.1: Field Map: (a) Drone footage (b) Generated map with waypoints

The navigation system requires a two-stage preprocessing procedure: mapping using drone footage and designating waypoints across the field, as shown in Figure ??. In the initial stage, a drone equipped with a camera is deployed to capture top-down images of the field. Specialized machine learning algorithm trained with previous years' corn field data then processes these images, generating a detailed digital map of the field. Following map creation, waypoints are identified and designated on the

map. These waypoints represent specific locations within the field that require sensor data collection, which is selected manually by the users.

For navigation, the AMIGA platform utilizes wheel odometry for local positioning and cross-checks with GPS signal for higher accuracy. One GPS signal receiver is set at a stationary location near the field and another one is placed on top of the AMIGA platform. By using real-time kinematic positioning, the navigation system is capable of achieving higher absolute position accuracy within 5m. This real-time localization capability ensures the robot reaches the designated waypoints on the field precisely, facilitating accurate navigation and ultimately successful sensor insertions.

7.1.2 Robot Manipulator xARM

For robot arm, the xARM6, a commercially available robotic arm with 6 degrees-of-freedom, was used to manipulate the gripper to the detected target cornstalk position and to the sensor replacement and calibration mechanisms. The xARM is attached to the front center of the mobile base facing downward towards the ground with the gripper attached as the end-effector. With this configuration, the base can straddle two rows of cornstalks and the xArm robot arm is positioned in the center of the rows.

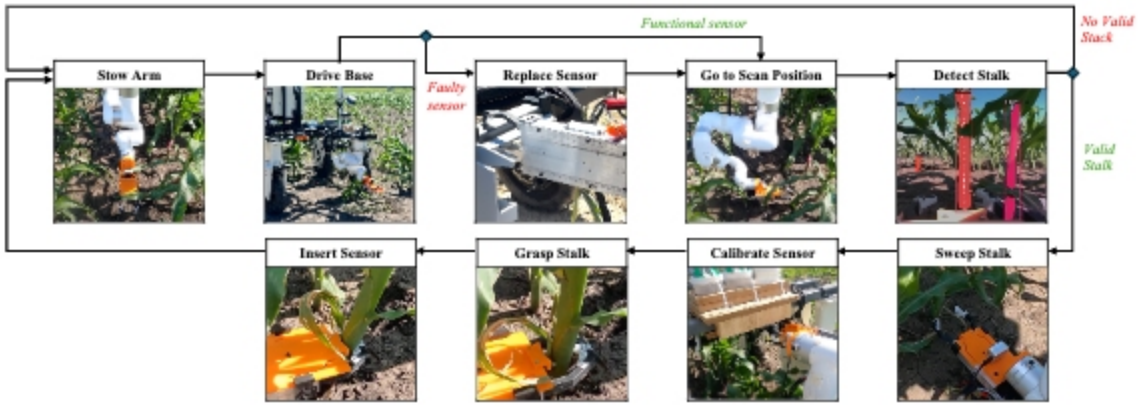

Figure 7.2: Sensor Insertion Motion

The xARM robotic arm follows a sequence of motion for cornstalk sensor insertion task as shown in Figure 7.2. When the insertion task is initiated, the arm is stowed facing forward to keep the arm safe when the mobile base is driving. The base drives

to the next waypoint, and if the sensor requires replacement, the arm moves to the replacement mechanism and swaps out the sensor. Then, the arm moves to the scan position, facing the right side toward the row of stalks. The the camera sensor detects for stalks, and when there is a valid stalk, the arm moves towards the stalk and executes a 30-degrees arc motion around it, as shown in Figure 7.3. The sweep motion is done to identify the optimal insertion angle, where the stalk's cross-sectional area is maximized. Prior to inserting the sensor, the gripper moves to the on-board sensor calibration mechanism to calibrate and clean the sensor. Finally, the xARM employs its gripper to securely hook the fingers around the stalk at the determined optimal angle and the gripper inserts the sensor.

Figure 7.3: Sweep Motion

7.2 In-lab Testing

Evaluation of the robotic system was conducted through a combination of controlled lab experiments and extensive field testing. In the lab, tests focused on verifying the functionality of individual subsystems, including the gripper's sensor insertion capabilities, the sensor replacement and calibration procedure, and the integration of

the navigation system. To complement limited field testing opportunities, in-lab tests were performed using mock cornstalks, greenhouse-grown cornstalks, and comparable vegetable products to simulate realistic conditions.

7.2.1 Gripper Sensor Insertion Testing

Figure 7.4: Gripper Insertion Testing: (a) Vegetable products of varying diameter (b) Gripper insertion testing using leek

To assess the linear actuator's force and stability for complete sensor insertion, a series of tests were conducted under static conditions with the mobile base immobilized. These tests, conducted throughout the development process, utilized a variety of commercially available vegetable products, including leek, green onion, celery, and cucumber, as proxies for cornstalks. The vegetable samples, representing a range of diameters, were employed to evaluate the gripper's adaptability to different crop dimensions. Results indicate successful sensor insertion for crop diameters spanning from 6.5mm to 32mm.

In addition, the cornstalk detection algorithm and the motion sequence of the robotic arm and gripper were tested using mock cornstalks and greenhouse-grown cornstalks. A small greenhouse was installed in the lab to grow cornstalks for controlled testing. Four cornstalks were grown biweekly following germination, emergence, and

Figure 7.5: Testing with corn: (a) Growing cornstalks in an indoor greenhouse (b) Testing perception insertion motion sequence with a mock cornstalk

transplant stages, and after 5 to 7 weeks, these cornstalks reached an appropriate size for sensor insertion testing. Both mock and greenhouse-grown cornstalks were used to evaluate the perception system's detection accuracy and the success of the insertion motion sequence.

7.2.2 xARM Manipulator Workspace Testing

Although the xARM6 robotic manipulator is a cost-effective solution, its motion control system has limitations in preventing encounters with singularities, joint angle limits, and speed constraints. When these conditions arise, the manipulator halts and requires reinitialization.

To mitigate these limitations and enhance operational efficiency, a scan position was established through trial and error. This scan position strategically positions the gripper camera to face the cornstalks while maintaining a joint configuration that avoids singularities and operates within safe joint angle and speed limits.

The manipulator's movements during sensor insertion follow a set order based on the cornstalk's detected location. To ensure consistent and reliable performance,

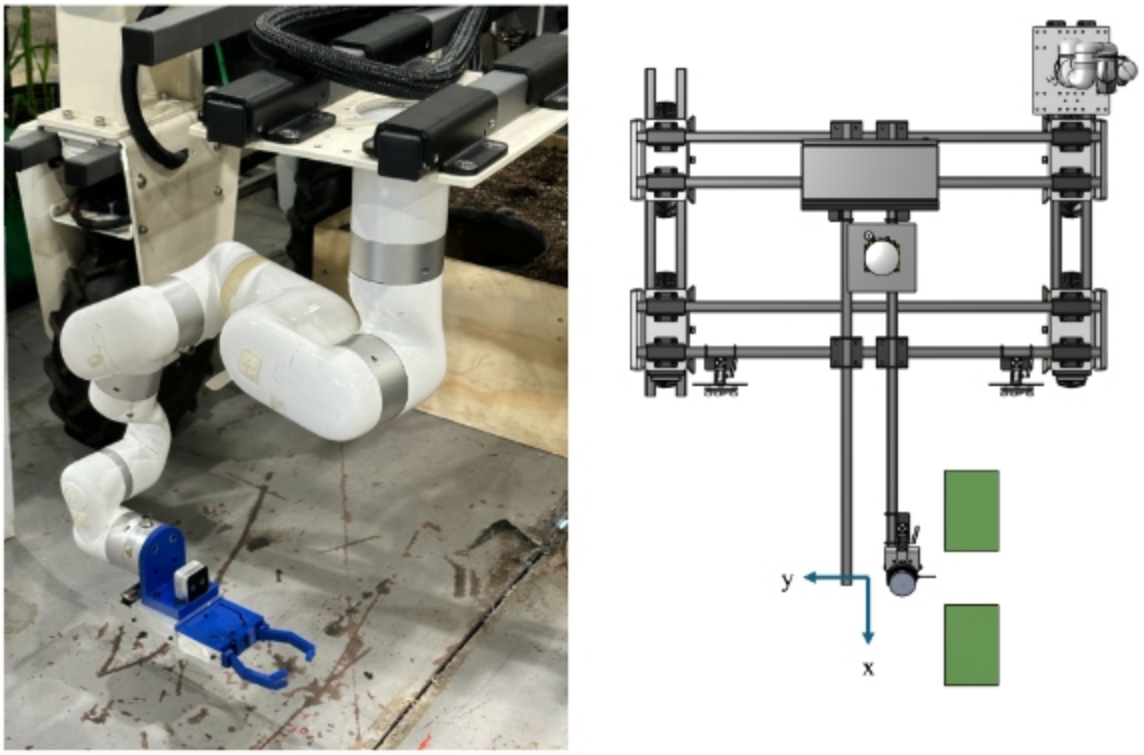

Figure 7.6: Manipulator Workspace: (a) Scan position (b) Top-down view of the xARM workspace

iterative testing was conducted to define the xARM's workspace, focusing on areas where the arm motions could be reliably executed. Cornstalks located within this defined workspace were selected for sensor insertion, which minimized motion failures.

	Workspace (m)			
	X		Y	Z
min	-0.4	0.1	-0.281	0.7
max	-0.1	0.4	-0.481	0.825

Table 7.1: Manipulator Workspace (unit in m)

7.2.3 Sensor Replacement Evaluation

To extensively evaluate the performance of the sensor replacement, the sensor exchange process was tested for 50 iterations. Each trial involved unloading the sensor from the

gripper into the retrieval box and loading a new sensor held in the sensor replacement mechanism. The sensor replacement mechanism holds 5 sensors, and each sensor was tested for 10 trials. Out of 50 iterations, the results showed that unloading and loading the sensor are highly reliable with a success rate of 100%.

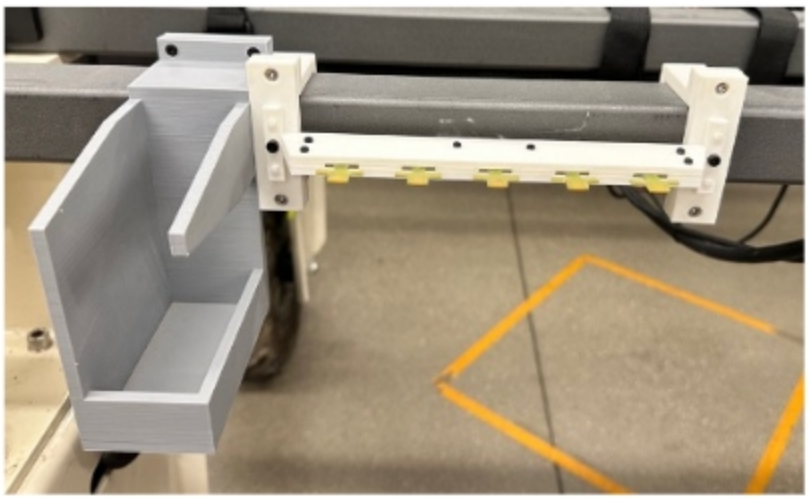

Figure 7.7: Sensor Replacement Ablation Setup

For comparison, an ablation study was conducted on a replacement mechanism without the funneling system. In this setup, the sensor holder lacked the T-shaped extrusion used for precise alignment, with all other experimental conditions remaining identical (see Fig. 7.7). Over 50 iterations, the success rate for both unloading and loading the sensor dropped to 24%, underscoring the effectiveness of the funneling mechanism with the T-shaped tapered extrusion in achieving reliable, precise alignment.

7.2.4 Sensor Calibration Evaluation

A total of 40 test runs were conducted across 25 sensors to evaluate the sensor calibration unit. Each run involved exposing the sensor to the three solutions for 15 seconds each. Common sensor failure cases are when the two calibration voltages are approximately the same or when the high-concentration nitrate solution is read as a higher voltage when expected to be lower. A successful calibration rate of 62.5% was determined by whether the sensor exhibited the expected behavior shown in Fig. 7.8(b).

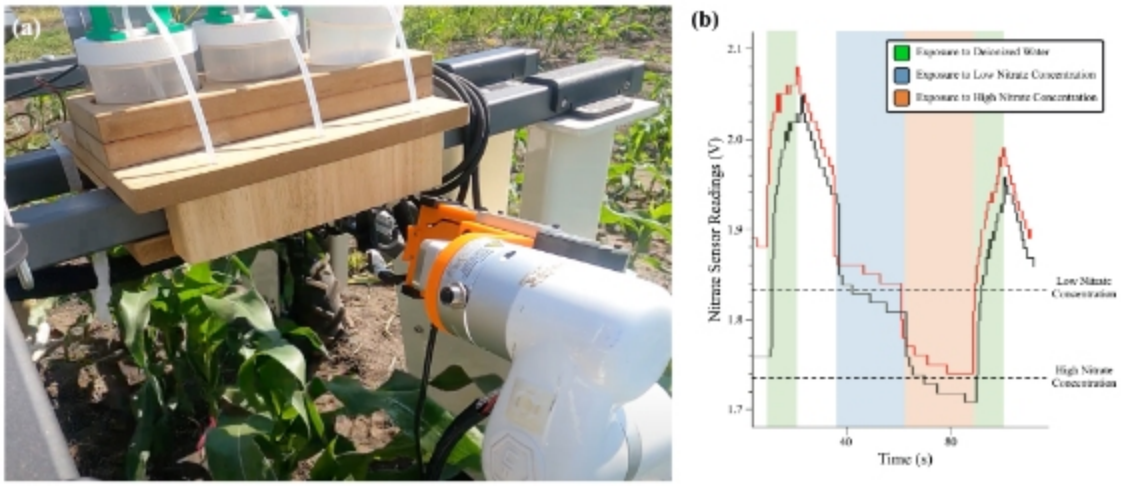

Figure 7.8: Expected Sensor Calibration Behavior

7.2.5 Navigation Integration Testing

Prior to field deployment, the navigation system and its integration with the sensor insertion system underwent testing within a controlled environment on the campus quad. This testing aimed to validate the navigation system's functionality and communication protocols in a field setting.

For these tests, the GPS coordinates of arbitrary waypoints were collected, and a navigation path was then generated based on the selected waypoint sequence. The robot autonomously followed the planned path, arriving at each waypoint as programmed. Upon reaching the final waypoint, the navigation system transmitted a pre-defined signal to the sensor insertion system, triggering the initiation of the insertion motion sequence. Once the insertion process was successfully completed, the insertion system reciprocated by sending a completion signal back to the navigation system. Through these comprehensive integration tests, the communication protocols between the navigation and sensor insertion subsystems were refined, ultimately enhancing the system's overall reliability and robustness.

Figure 7.9: (a) Navigation Integration testing on campus quad (b) Planned path based on the waypoints

7.3 Field Testing

Field tests assessed the system's overall robustness and reliability in diverse agricultural conditions.

7.3.1 Rivendale Farm

The initial cornfield test was conducted at Rivendale Farm, a local farm at Pittsburgh. This cornfield test, while achieving only one successful sensor insertion out of ten insertion attempts, provided valuable insights. The cornfield presented two primary challenges: uneven terrain and irregular plant spacing. Due to the uneven terrain, the sensor insertion motion pipeline struggled with the manipulator attempting to insert sensor higher on the cornstalks, leading to self collision. Additionally, mechanical challenges arose with a broken gripper mount and power supply connection damage. These mechanical issue were later resolved by machining aluminum

Figure 7.10: Rivendale Farm: (a) Cornstalk Field Drone Footage (b) Field Testing

gripper mount and changing electric connection to more reliable Anderson connector. Lastly, navigation performance was satisfactory on flat terrain, but uneven ground caused concerning path deviations. In conclusion, the initial field test at Rivendale Farm exposed critical challenges in terrain navigation, sensor placement, and system durability, necessitating comprehensive system refinements to achieve reliable and robust field performance. But, through the initial testing and failures, it prepared the robotic system better for the field testing at the Iowa Ames Curtis Farm.

7.3.2 Iowa Ames Curtis Farm

Field testing at the Iowa Ames Curtis Farm, in collaboration with Iowa State University, provided a platform to evaluate the robotic system for monitoring nitrate level in cornstalks under real-world agricultural conditions. To evaluate the robot's overall performance, the success rate of each subsystem was assessed. Post-insertion analysis, including depth and height measurements, provided critical insights into the accuracy and effectiveness of the sensor insertion process.

Cornstalk Dimensions

Concurrent with system evaluation, comprehensive measurements of cornstalk dimensions were collected to establish a detailed characterization of the target crops. The target cornstalk for nitrate monitoring are ones in the growth stage of V6 - V8.

Figure 7.11: Testing at Curtis Farm

Average Cornstalk Dimensions (mm)		
Minor Axis	Major Axis	Height
17.8	23.2	565

Table 7.2: Average Cornstalk Dimensions

Due to the variation of corn growth, there are wide range of cornstalk diameter and height. To obtain a detailed characterization of the target cornstalks, the cornstalk dimensions for 40 random cornstalk were collected. As shown in the following table, the average minor and major axis are 17.8 mm and 23.2 mm, respectively. In addition, the average height was 56.5 cm.

Insertion Process Evaluation

The sensor insertion task was tested on 30 different cornstalks at the field. For the evaluation, the metric consists of 5 criteria involving robot evaluation and manual post-trial evaluation.

The insertion motion sequence is mainly detecting a target cornstalk followed by grasping the stalk and inserting the sensor. The success of these three motion steps were evaluated for the robot evaluation. The stalk detection resulted in 97% success rate, with only a single failure case out of 30 trials where a leaf was detected as a stalk, as shown in Fig. 7.13. Whenever the stalk was detected, the robot was able to grasp the stalk in between the gripper fingers, indicating a successful and reliable arm motion sequence. Out of the 29 cases where the stalk was successfully grasped,

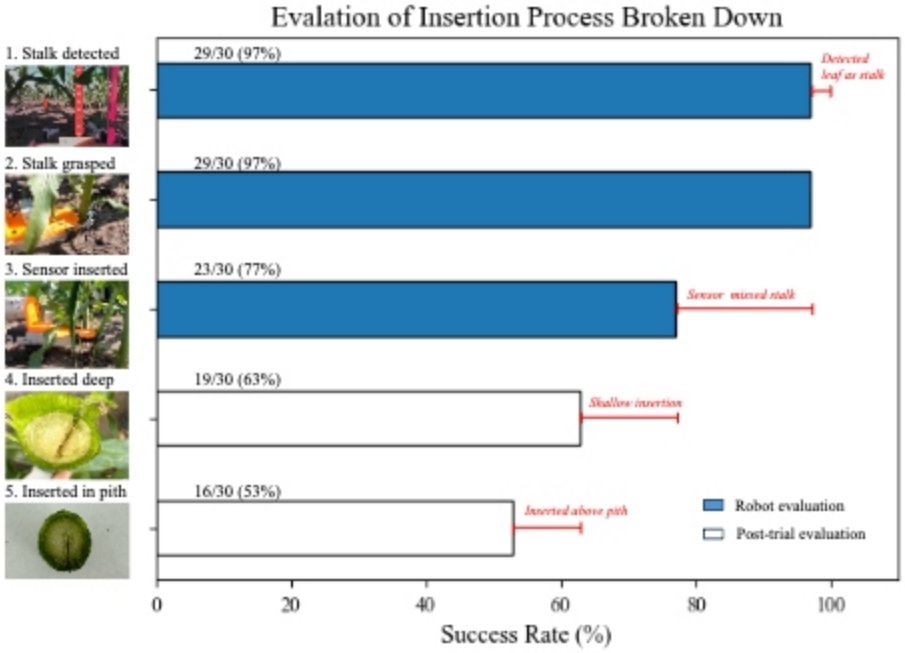

Figure 7.12: Overall performance of sensor insertion evaluated on 30 field cornstalks.

the sensor insertion was successful for 23 stalks, resulting in a progressive success rate of 77%. The cause of the failure cases were the misalignment between the sensor and the center of the stalk.

After the sensor insertion, it is necessary to determine if the insertion is deeper than 8.5 mm in the pith region. This evaluation was done after the insertion by slicing the cornstalk horizontally at the insertion height. By measuring the depth of the insertion, we were able to verify that there were 19 successful insertions with sufficient depth, resulting in a collective success rate of 63%. Sensor misalignment with the stalk's center was the primary cause of failures, as shown in Fig. 7.13. Among the 19 successful sensor insertions, 16 sensors were inserted in the pith region, which gives a final overall success rate of 53% for the sensor insertion. This is an improvement compared to 31% overall success rate of crop monitoring robot developed by Lee et al. [21].

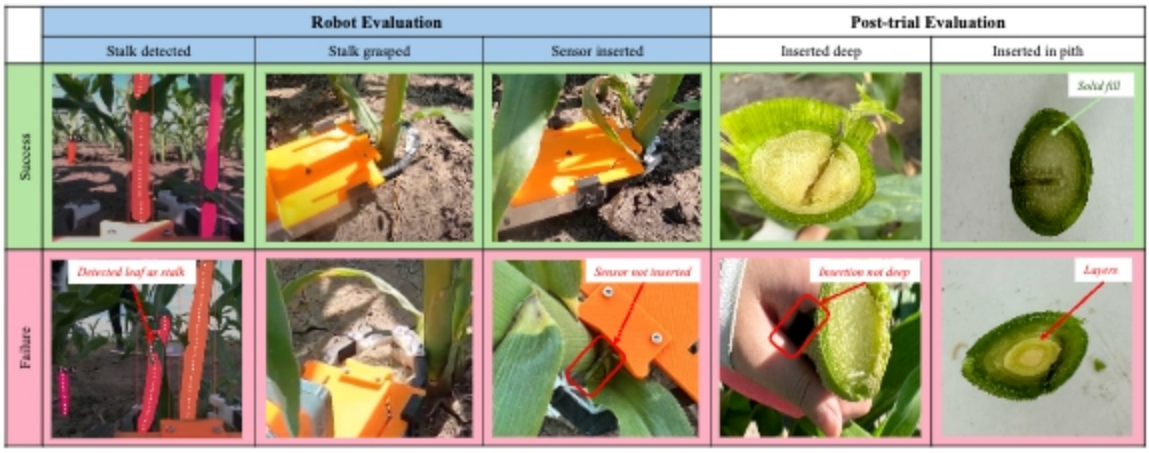

Figure 7.13: Examples of success and failure cases for each of the criteria for the sensor insertion evaluation.

Baseline Comparison

The current gripper design exhibits significant improvements in sensor insertion performance compared to the previous version developed by Lee et al. [21] (Fig. 7.14). The previous gripper design utilizes a C-shaped funnel for aligning the cornstalk to the center prior to sensor insertion and uses V-sliding block and spring mechanism for sensor insertion (see [21] for more details). The advancements in both the sensing and actuation mechanisms have led to higher success rates across all evaluation criteria.

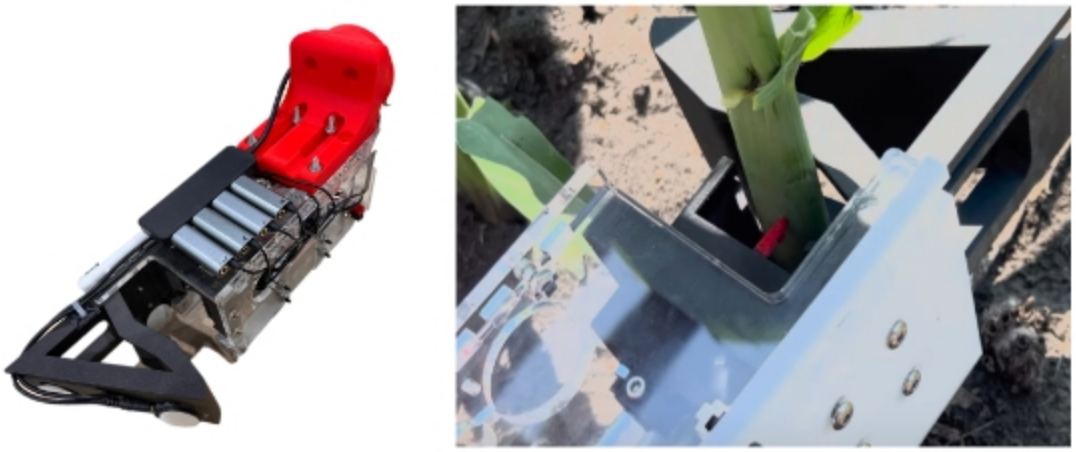

Figure 7.14: Previous Gripper Design

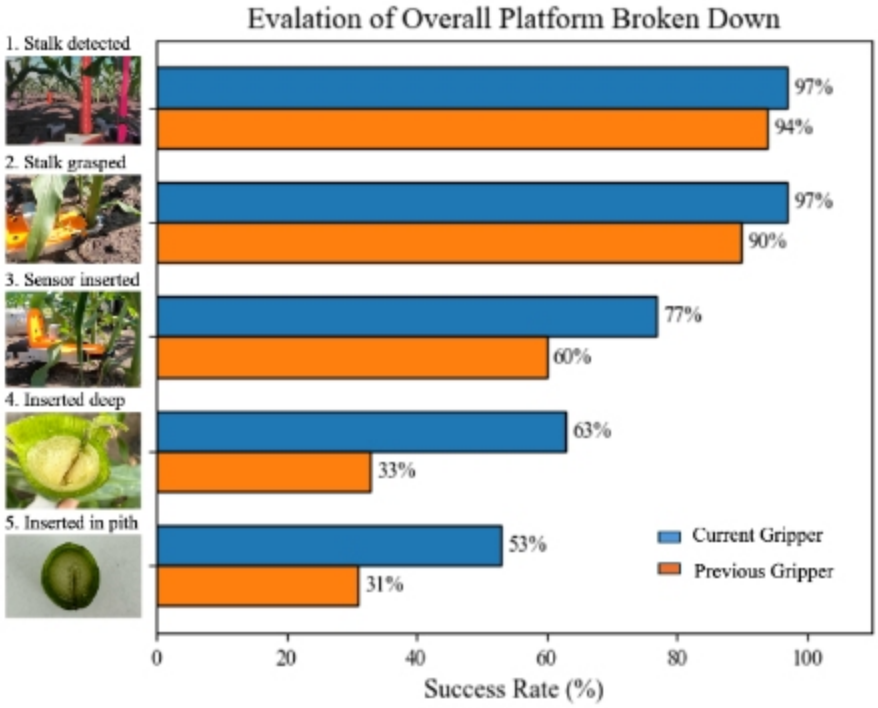

Figure 7.15: Sensor Insertion Performance Baseline Comparison

One of the key improvements is the enhanced stalk grasp motion, achieving a 97% success rate, up from the previous 90% (see Fig 7.15). The refined arm motion, incorporating a predefined workspace and optimized gripper design, resulted in consistently flawless grasping. This demonstrates the significant advancements in mechanical control and precision of the gripper. Furthermore, the sensor insertion process, a critical aspect of the system, saw substantial improvement. The current gripper achieved a 77% insertion success rate, a marked increase from the previous 60%. The two-finger design and coupled sliding mechanism notably reduced misalignment issues that were more frequent in earlier iterations.

Post-trial evaluations further underscored the system's advancements. The current design achieved a 63% success rate in insertions reaching the required depth, a significant improvement from the 33% success rate of the previous gripper. Additionally, 53% of the sensors were accurately placed within the pith region, compared to 31% in the prior version. These improvements in sensor alignment and depth control

demonstrate the system's enhanced precision and effectiveness in achieving the desired insertion accuracy in field conditions.

As illustrated in Fig. 7.15, the performance gains in the current gripper design are evident across all phases of the sensor insertion process. This progression highlights how refinements in grasping and insertion mechanisms contribute to a more reliable and efficient sensor insertion.

7.4 Visual Servoing Evaluation at Hazelwood

To evaluate the visual servoing implementation described in Section 6, testing was conducted in October 2024 at Hazelwood, Pittsburgh. During these tests, the nitrate sensor was inserted into 30 different cornstalks using visual servoing, and metrics such as insertion success rate and distance from the vertical center were recorded. Of the 30 trials, 24 insertions were successful, yielding an 80% success rate. This marks a modest improvement over the 77% success rate achieved in field tests at Iowa Ames Curtis Farm (refer to Section 7.3.2), where open-loop control was employed rather than visual servoing, though the difference is not statistically significant.

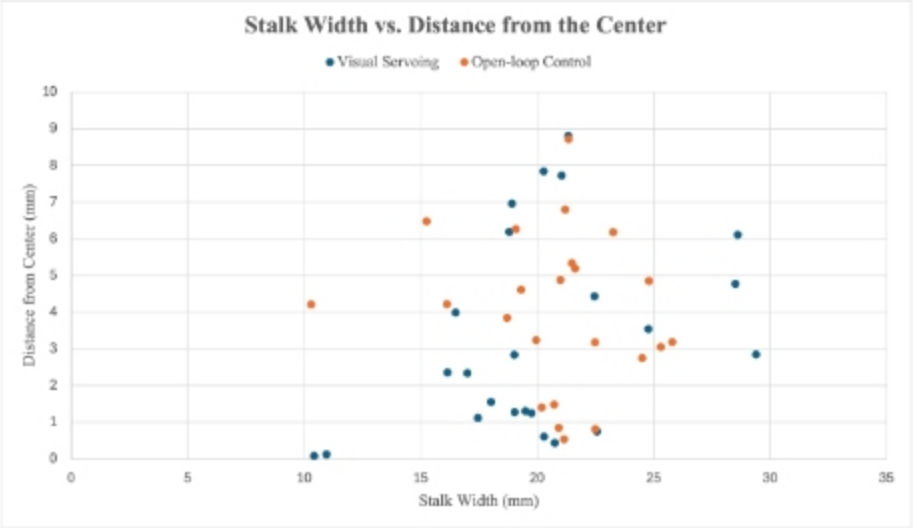

Figure 7.16: Comparing Open-loop and Visual Servoing

To further evaluate precision, the distance between the sensor insertion location and the center of the cornstalk was measured, as illustrated in Figure 7.16. Sensor

insertions performed with the visual servoing implementation achieved an average distance of 3.30 mm from the center, with a median of 2.60 mm. In contrast, insertions conducted with open-loop control at Ames Curtis Farm resulted in an average distance of 4.00 mm and a median of 4.21 mm. These findings indicate that the visual servoing control strategy enabled more precise insertions closer to the cornstalk center.

Figure 7.17: Close-up Detection Failure Cases

A key limitation observed with the visual servoing implementation was the segmentation mask's inability to accurately identify stalks as polygons at close range. The segmentation model used for stalk detection, Mask R-CNN, performed highly effectively at detecting stalks from a distance (achieving a 97% success rate, as shown in Fig. 7.12), but struggled to maintain this accuracy when detecting stalks up close, as illustrated in Fig. 7.17. This often led to increased alignment errors. The rectangular segmentation mask worked well when the stalk was farther away from the camera. However, at closer range, the camera captures only a small section of the stalk, which may include protruding leaves. In these close-up cases, a polygon-shaped segmentation would have been more effective for accurate detection. Enhancing the segmentation model by training it with more close-up views of stalks and incorporating a greater variety of stalk appearances, including variations in leaf

structures, is anticipated to improve the visual servoing implementation's effectiveness and ultimately increase the insertion success rate.

Chapter 8

Conclusions

8.1 Summary

The results of the field evaluation demonstrated a successful robotic system and gripper for sensor insertion and replacement. The two-finger design allowed the gripper to grasp the stalk by moving forward in a straight line with the camera sensor viewing the stalk. When the stalk was successfully detected, the arm manipulation and gripper grasp motion was successful with no failure cases, indicating effective manipulator motion sequence and gripper design. The gripper was compact in size using the single-actuator coupled sliding mechanism, and this design allowed the sensor to be inserted very close to the ground to reach the pith region.

The sensor replacement process demonstrated the exceptional reliability for unloading and loading sensors, achieving a 100% success rate. These evaluations suggest that our approach offers a cost-effective and mechanically simple solution for robotic applications demanding high-precision insertions with low-precision manipulators.

The primary cause of sensor insertion failures (10 out of 30 cases) at the field was sensor misalignment that resulted in missed or shallow insertions. This motivated the development of a closed loop vision-based robot arm control to center the gripper with high accuracy and precision prior to insertion.

The visual servoing implementation improved the robotic system's alignment accuracy for sensor insertions, achieving an 80% insertion success rate over previous open-loop control method that resulted in 77% success. By using vision-based control

to center the gripper on the cornstalk, the system achieved precise sensor placement, as validated by accurate distance measurements from the stalk center.

Current robot system replaces the sensor after 5 insertion iterations, but for future works, implementing automatic sensor fault detection would further improve the reliability of the sensor readings of this system. The sensor calibration evaluation showed the desired convergence pattern with a success rate of 63%. These failures were not evenly distributed and 47% of these failures occurred in the fourth quarter of testing. This increased failures are due to the expected wear and tear of interactive sensors [9] after multiple insertions.

8.2 Future Work

While the current system demonstrated successful sensor insertion and replacement, there are several areas for improvement and further research to enhance its functionality, robustness, and applicability. This section suggests some of the key future directions.

Accurate detection of the pith region is essential for improving the precision of sensor insertions. Currently, the system aims to reach as low as possible to insert the sensor in the pith region, but this approach is not consistent because the ground could be leveled or there could be obstacles, such as stones. Future work should focus on developing advanced vision or sensor-based algorithms that can reliably identify the pith region across varying cornstalks and environmental conditions. This could include employing more sophisticated machine learning techniques, such as sample-based learning, to train models capable of recognizing the pith region based on visual and structural cues from diverse cornstalk samples. These improvements would enable more precise and consistent insertions, even in complex or dynamic field environments.

The current system is optimized for flat terrain, but real-world environments often include sloped or uneven surfaces. Field testing at Rivendale has shown that the current manipulator control is not effective on slopes, often resulting in singularities or exceeding joint limits. Future research should address the challenge of arm manipulation on sloped terrains. This could involve developing adaptive control algorithms that allow the robotic arm to adjust its position and orientation

in response to the terrain, while also avoiding singularities and joint limit violations.

To enhance the visual servoing implementation, future work should focus on improving close-range stalk detection and alignment accuracy. While the current model effectively detects stalks from a distance, closer views reveal limitations, particularly with obstructions like leaves. Training the segmentation model with more diverse, close-up samples of cornstalks—including variations in leaf structure—would improve detection and enable more accurate sensor insertions. Further advancements could also explore adaptive visual servoing techniques, allowing the system to dynamically adjust based on real-time feedback about environmental conditions, such as changes in lighting or stalk orientation. By refining these aspects, future implementations will achieve greater precision and robustness.

The system currently lacks an implementation to autonomously detect sensor faults and currently replaces the sensor after a set number of insertions. Implementing automatic fault detection would greatly improve the reliability and longevity of the system. Future work should focus on implementing rule-based fault detection systems that can monitor sensor performance in real-time. This implementation could trigger automatic sensor replacement when faults are detected, leading to more efficient operation and reliable sensor reading across multiple sensor insertions.

By addressing these areas, future iterations of the system can achieve greater precision, reliability, and adaptability, making it a viable solution for widespread agricultural automation and other sensor-based applications.

Chapter 9

Appendix

General Advice for Robotic Design

Here are key principles and practical advice for tackling robotic design challenges from insights I gained from this research project. These insights cover essential aspects of the design process, from understanding requirements to testing and iterative development.

1. **Understand the Research Problem Thoroughly**: Gain a clear understanding of the research problem, including its requirements and constraints. For design challenges with multiple requirements—such as compact size, adaptability, and precision—it is crucial to comprehend all aspects upfront. If requirements evolve or change during the development process, it may necessitate restarting the design and fabrication.
2. **Research Existing Solutions**: Investigate existing products and mechanisms that can be adapted for your design problem. For example, identifying a suitable battery connector enabled the sensor modification for autonomous sensor exchange. Similarly, the sliding mechanism described in [16] was modified and incorporated into the gripper design.
3. **Maintain an Open-Minded Approach**: Consistently brainstorm ideas and stay open-minded when addressing challenges. Everyday objects can serve as sources of inspiration. For instance, the sensor lever mechanism was inspired by

a pair of scissors, while the compliant finger pad design drew inspiration from car wheel spokes.

4. **Embrace Iterative Design**: Treat design as an iterative process that involves concept sketching, prototyping for proof-of-concept, and modification. In the gripper development process, designs were created using CAD, prototyped with a 3D printer, and tested at the subunit level. Based on testing results, the designs were adjusted multiple times to refine tolerances and to adjust parameters.
5. **Develop Proficiency in 3D CAD**: Acquiring 3D CAD skills is essential for visualizing ideas, facilitating the initial proof-of-concept step, and effectively communicating designs with others.
6. **Collaborate and Seek Expert Advice**: Share your ideas with experts and solicit feedback. Valuable support can enhance various aspects of the project, such as electronics design, sensor integration, and specific fabrication techniques like rubber casting.
7. **Hone Fabrication Skills**: Strengthen your fabrication skills, as they directly influence your approach to problem-solving and solution development. In the gripper project, skills in 3D printing, Arduino programming, and metal fabrication were instrumental. Additionally, new skills, such as PCB design, were acquired during the process.
8. **Adopt a "Simple Yet Effective" Philosophy**: Focus on simplicity and efficiency in design. Avoid adding unnecessary actuators or mechanisms that could introduce errors or increase uncertainty. For example, in the gripper design, initially for the sensor lever, adding an additional actuator for hooking and unhooking the sensor was considered. For the precise alignment, implementing visual detection for sensor exchange was considered. However, this could introduce unwanted uncertainty, and thus, the linear movement of the existing top slider and a T-shaped hole within the gripper were utilized effectively.
9. **Address Requirements Sequentially**: When designing interconnected parts for systems with multiple requirements, tackle one requirement at a time. This approach simplifies development and avoids overwhelming complexity. For

the gripper, the development sequence was: 1) designing finger movement, 2) incorporating a sensor lever for engagement and disengagement, and 3) integrating a funneling mechanism for sensor exchange.

10. **Test Throughout Development**: Conduct rigorous testing throughout the development process to ensure functionality. Develop subsystem testing methods to validate each step. For the gripper, individual components like the linear actuator, finger control, sensor hooking mechanism, and sensor exchange functionality were tested separately before integration and full assembly.

Bibliography

[1] Md Azahar Ali, Xinran Wang, Yuncong Chen, Yueyi Jiao, Navreet K Mahal, Satyanarayana Moru, Michael J Castellano, James C Schnable, Patrick S Schnable, and Liang Dong. Continuous monitoring of soil nitrate using a miniature sensor with poly (3-octyl-thiophene) and molybdenum disulfide nanocomposite. *ACS applied materials & interfaces*, 11(32):29195–29206, 2019. 2.1

[2] Ron Berenstein, Averell Wallach, Pelagie Elimbi Moudio, Peter Cuellar, and Ken Goldberg. An open-access passive modular tool changing system for mobile manipulation robots. In *2018 IEEE 14th International Conference on Automation Science and Engineering (CASE)*, pages 592–598. IEEE, 2018. 2.2

[3] Andrea Botta, Paride Cavallone, Lorenzo Baglieri, Giovanni Colucci, Luigi Tagliavini, and Giuseppe Quaglia. A review of robots, perception, and tasks in precision agriculture. *applied mechanics*, 3(3):830–854, 2022. 1.1, 2.1

[4] Duke M Bulanon, Colton Burr, Marina DeVlieg, Trevor Braddock, and Brice Allen. Development of a visual servo system for robotic fruit harvesting. *AgriEngineering*, 3(4):840–852, 2021. 2.4

[5] Nikhil Chavan-Dafle, Matthew T Mason, Harald Staab, Gregory Rossano, and Alberto Rodriguez. A two-phase gripper to reorient and grasp. In *2015 IEEE International Conference on Automation Science and Engineering (CASE)*, pages 1249–1255. IEEE, 2015. 2.2

[6] Fei Chen, Kosuke Sekiyama, Baiqing Sun, Pei Di, Jian Huang, Hironobu Sasaki, and Toshio Fukuda. Design and application of an intelligent robotic gripper for accurate and tolerant electronic connector mating. *Journal of Robotics and Mechatronics*, 24(3):441, 2012. 2.3

[7] Joseph Davidson, Santosh Bhusal, Changki Mo, Manoj Karkee, and Qin Zhang. Robotic manipulation for specialty crop harvesting: A review of manipulator and end-effector technologies. *Global Journal of Agricultural and Allied Sciences*, 2(1):25–41, 2020. 2.1

[8] Daniele De Gregorio, Riccardo Zanella, Gianluca Palli, Salvatore Pirozzi, and Claudio Melchiorri. Integration of robotic vision and tactile sensing for wire-

terminal insertion tasks. *IEEE Transactions on Automation Science and Engineering*, 16(2):585–598, 2018. 2.3

[9] Sumaira Ghazal, Arslan Munir, and Waqar S Qureshi. Computer vision in smart agriculture and precision farming: Techniques and applications. *Artificial Intelligence in Agriculture*, 2024. 2.1

[10] Dominic Guri, Moonyoung Lee, Oliver Kroemer, and George Kantor. Hefty: A modular reconfigurable robot for advancing robot manipulation in agriculture. *arXiv preprint arXiv:2402.18710*, 2024. 2.5, 7.1.1

[11] Koichi Hashimoto. *Visual servoing: real-time control of robot manipulators based on visual sensory feedback*, volume 7. World scientific, 1993. 2.4

[12] Hussam Ibrahim, Shihao Yin, Satyanarayana Moru, Yunjiao Zhu, Michael J Castellano, and Liang Dong. In planta nitrate sensor using a photosensitive epoxy bioresin. *ACS Applied Materials & Interfaces*, 14(22):25949–25961, 2022. 1.2, 2.1, 2.1.1, 3.2, 3.3, 5.6

[13] Natsuki Ikeda, Ryo Shigeta, Junichiro Shiomi, and Yoshihiro Kawahara. Soil-monitoring sensor powered by temperature difference between air and shallow underground soil. *Proceedings of the ACM on Interactive, Mobile, Wearable and Ubiquitous Technologies*, 4(1):1–22, 2020. 2.1

[14] Ramón Isla and Alfred M Blackmer. A simplified test of cornstalk nitrate for better n management. *Agronomy for sustainable development*, 27:237–241, 2007. 3.2

[15] Farrokh Janabi-Sharifi, Lingfeng Deng, and William J Wilson. Comparison of basic visual servoing methods. *IEEE/ASME Transactions on Mechatronics*, 16 (5):967–983, 2010. 2.4

[16] Merritt Jenkins. Detecting and grasping sorghum stalks in outdoor occluded environments. Master's thesis, Carnegie Mellon University, Pittsburgh, PA, August 2017. 2.5, 2

[17] Wei Ji, Dean Zhao, Fengyi Cheng, Bo Xu, Ying Zhang, and Jinjing Wang. Automatic recognition vision system guided for apple harvesting robot. *Computers & Electrical Engineering*, 38(5):1186–1195, 2012. 2.1

[18] Ville Kankare, Markus Holopainen, Mikko Vastaranta, Eetu Puttonen, Xiaowei Yu, Juha Hyyppä, Matti Vaaja, Hannu Hyyppä, and Petteri Alho. Individual tree biomass estimation using terrestrial laser scanning. *ISPRS Journal of Photogrammetry and Remote Sensing*, 75:64–75, 2013. 2.1

[19] Jonathan Kelly, Jared L Crain, and WR Raun. By-plant prediction of corn (zea mays l.) grain yield using height and stalk diameter. *Communications in Soil Science and Plant Analysis*, 46(5):564–575, 2015. 3.4

[20] Alexander Kirillov, Eric Mintun, Nikhila Ravi, Hanzi Mao, Chloe Rolland, Laura Gustafson, Tete Xiao, Spencer Whitehead, Alexander C. Berg, Wan-Yen Lo, Piotr Dollár, and Ross Girshick. Segment anything, 2023. URL `https://arxiv.org/abs/2304.02643`. 6.1

[21] Moonyoung Lee, Aaron Berger, Dominic Guri, Kevin Zhang, Lisa Coffey, George Kantor, and Oliver Kroemer. Towards autonomous crop monitoring: Inserting sensors in cluttered environments. *IEEE Robotics and Automation Letters*, 2024. 2.5, 6, 7.3.2, 7.3.2

[22] Nan Li, Xiaoguang Zhang, Chunlong Zhang, Luzhen Ge, Yong He, and Xinyu Wu. Review of machine-vision-based plant detection technologies for robotic weeding. In *2019 IEEE International Conference on Robotics and Biomimetics (ROBIO)*, pages 2370–2377. IEEE, 2019. 2.1

[23] Jun Liu, Haotian Cai, Shan Chen, Jie Pi, and Liye Zhao. A review on soil nitrogen sensing technologies: challenges, progress and perspectives. *Agriculture*, 13(4):743, 2023. 2.1.1

[24] Shoufeng Liu, Fujun Wang, Zhu Liu, Wei Zhang, Yanling Tian, and Dawei Zhang. A two-finger soft-robotic gripper with enveloping and pinching grasping modes. *IEEE/ASME Transactions on Mechatronics*, 26(1):146–155, 2020. 2.2

[25] Navreet K Mahal, Fernando E Miguez, John E Sawyer, Liang Dong, Patrick S Schnable, and Michael J Castellano. Stalk sap nitrate test as a potential tool for nitrogen fertilizer recommendations for maize. *Field Crops Research*, 310:109330, 2024. 2.1.1

[26] Marco Mora, Felipe Avila, Marcos Carrasco-Benavides, Gonzalo Maldonado, Jeissy Olguín-Cáceres, and Sigfredo Fuentes. Automated computation of leaf area index from fruit trees using improved image processing algorithms applied to canopy cover digital photograpies. *Computers and Electronics in Agriculture*, 123:195–202, 2016. 2.1

[27] Andrew S Morgan, Bowen Wen, Junchi Liang, Abdeslam Boularias, Aaron M Dollar, and Kostas Bekris. Vision-driven compliant manipulation for reliable, high-precision assembly tasks. *arXiv preprint arXiv:2106.14070*, 2021. 2.3

[28] Tim Mueller-Sim, Merritt Jenkins, Justin Abel, and George Kantor. The robotanist: A ground-based agricultural robot for high-throughput crop phenotyping. In *2017 IEEE international conference on robotics and automation (ICRA)*, pages 3634–3639. IEEE, 2017. 2.2, 4.2

[29] Kaidi Nie, Weiwei Wan, and Kensuke Harada. An adaptive robotic gripper with l-shape fingers for peg-in-hole tasks. In *2018 IEEE/RSJ International Conference on Intelligent Robots and Systems (IROS)*, pages 4022–4028. IEEE, 2018. 2.3

[30] Yonghyun Park, Jaehwi Seol, Jeonghyeon Pak, Yuseung Jo, Changjo Kim, and

Hyoung Il Son. Human-centered approach for an efficient cucumber harvesting robot system: Harvest ordering, visual servoing, and end-effector. *Computers and Electronics in Agriculture*, 212:108116, 2023. 2.4

[31] Jie Ren, Ning Kong, Yuan Zhuang, Jie Zhang, Shuai Ma, Bo Wang, and Wei Liu. A review on the interfaces of orbital replacement unit: Great efforts for modular spacecraft. *Proceedings of the Institution of Mechanical Engineers, Part G: Journal of Aerospace Engineering*, 235(14):1941–1967, 2021. 2.2

[32] Natalia Rogovska, David A Laird, Chien-Ping Chiou, and Leonard J Bond. Development of field mobile soil nitrate sensor technology to facilitate precision fertilizer management. *Precision agriculture*, 20:40–55, 2019. 2.1.1

[33] Antonio Rosales, Tapio Heikkilä, and Markku Suomalainen. Visual servoing based on 3d features: Design and implementation for robotic insertion tasks. *arXiv preprint arXiv:2405.18830*, 2024. 2.4

[34] Uferah Shafi, Rafia Mumtaz, José García-Nieto, Syed Ali Hassan, Syed Ali Raza Zaidi, and Naveed Iqbal. Precision agriculture techniques and practices: From considerations to applications. *Sensors*, 19(17):3796, 2019. 1.1, 2.1

[35] Nikolaus Vahrenkamp, Steven Wieland, Pedram Azad, David Gonzalez, Tamim Asfour, and Rudiger Dillmann. Visual servoing for humanoid grasping and manipulation tasks. In *Humanoids 2008-8th IEEE-RAS International Conference on Humanoid Robots*, pages 406–412. IEEE, 2008. 2.4

[36] Nicolas Virlet, Kasra Sabermanesh, Pouria Sadeghi-Tehran, and Malcolm J Hawkesford. Field scanalyzer: An automated robotic field phenotyping platform for detailed crop monitoring. *Functional plant biology*, 44(1):143–153, 2016. 2.1

[37] Achim Walter, Raghav Khanna, Philipp Lottes, Cyrill Stachniss, Roland Siegwart, Juan Nieto, and Frank Liebisch. Flourish-a robotic approach for automation in crop management. In *Proceedings of the international conference on precision agriculture (ICPA)*, 2018. 2.1

[38] Baohua Zhang, Yuanxin Xie, Jun Zhou, Kai Wang, and Zhen Zhang. State-of-the-art robotic grippers, grasping and control strategies, as well as their applications in agricultural robots: A review. *Computers and Electronics in Agriculture*, 177: 105694, 2020. 2.2